



Ice flow dynamics of the northwestern Laurentide Ice Sheet during the last deglaciation

Benjamin J. Stoker^{1*}, Helen E. Dulfer^{1,2}, Chris R. Stokes³, Victoria H. Brown³, Christopher D. Clark², Colm Ó Cofaigh³, David J.A. Evans³, Duane Froese⁴, Sophie L. Norris⁵ and Martin Margold^{1*}

5 1 Department of Physical Geography and Geoecology, Faculty of Science, Charles University in Prague, Albertov 6, 12800, Praha, Czech Republic.

2 Department of Geography, The University of Sheffield, Sheffield S102TN, UK.

3 Department of Geography, Durham University, Durham, United Kingdom.

4 Department of Earth and Atmospheric Sciences, Faculty of Science, University of Alberta, Edmonton, AB, Canada.

5 Department of Geography, David Turpin Building, University of Victoria, Victoria, V8P 5C2, British Columbia, Canada.

10 *Correspondence to:* Benjamin J. Stoker (stokerb@natur.cuni.cz) or Martin Margold (margold@natur.cuni.cz)

Abstract. Reconstructions of palaeo-ice stream activity provide an insight into the processes governing ice stream evolution over millennial timescales. The northwestern sector of the Laurentide Ice Sheet experienced a period of rapid retreat driven by warming during the Bølling–Allerød (14.7 – 12.9 ka) which may have contributed significantly to global mean sea level rise during this time. It therefore provides an opportunity to investigate ice sheet dynamics during a phase of rapid ice sheet retreat.

15 Here, we classify coherent groups of ice flow parallel lineations into 326 flowsets and then categorise them as ice stream, deglacial, inferred deglacial or event type flowsets. Combined with ice marginal landforms and a new ice margin chronology (Dalton et al., 2023), we present the first reconstruction of ice flow dynamics of the northwestern Laurentide Ice Sheet at 500-year timesteps through the last deglaciation. At the local Last Glacial Maximum (17.5 ka), the ice stream network was dominated by large, marine-terminating ice streams (>1000 km long) that were fed by the Laurentide–Cordilleran ice saddle

20 to the south and the Keewatin Ice Dome to the east. As the ice margin retreated onshore, the drainage network was characterised by shorter, land-terminating ice streams (<200 km long), with the exception of the Bear Lake and Great Slave Lake ice streams (~600 km long) that terminated in large glacial lakes. Rapid reorganisation of the ice drainage network, from predominantly northerly ice flow to westerly ice flow, occurred over ~2000 years, coinciding with a period of rapid ice sheet surface lowering in the ice saddle region. We note a peak in ice stream activity during the Bølling–Allerød that we suggest is a result of increased

25 ablation and a steepening of the ice surface slope in ice stream onset zones and the increase in driving stresses which contributed to rapid ice drawdown. The subsequent cessation of ice stream activity by the end of the Bølling–Allerød was a result of ice drawdown lowering the ice surface profile, reducing driving stresses and leading to widespread ice stream shut-down.

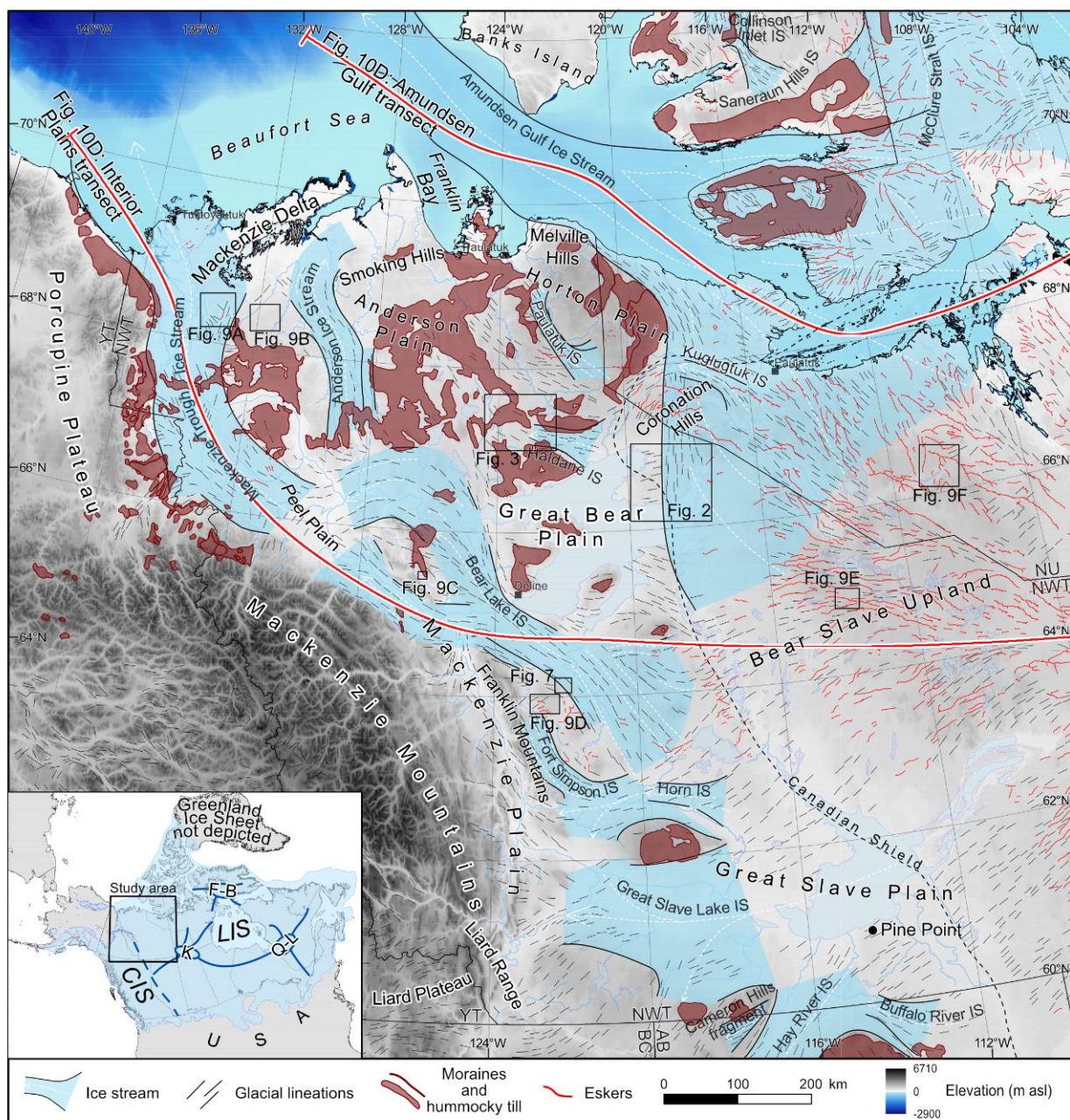


30 **1 Introduction**

Ice streams are narrow regions of fast flowing ice that exert an important influence on ice sheet mass balance by drawing down ice to lower elevations, where it is lost through melting (surface or basal) or calving (Bamber et al., 2000; Bennett, 2003; Robel and Tziperman, 2016). As such, ice streams are a key process in numerical models to project the future evolution of contemporary ice sheets (Gandy et al., 2019). The geomorphological record created by Late Quaternary ice sheets provides a
35 valuable opportunity to investigate ice stream dynamics, including the controls on ice stream activation, acceleration and shut-down (Winsborrow et al., 2010; Margold et al., 2018; Stokes et al., 2016). Crucially, the palaeoglaciological record allows us to investigate these systems over much longer timescales (1000s of years) than the contemporary observational record (10s of years) (Stokes et al., 2016; Gandy et al., 2019). The Laurentide Ice Sheet (LIS) was the largest component of the North
40 American Ice Sheet Complex, which also included the Cordilleran Ice Sheet (CIS) and Innuitian Ice Sheet, during the last glaciation (Dyke et al., 2002, 2003; England et al. 2006; Seguinot et al. 2016; Stokes, 2017; Dalton et al., 2023). At the Last Glacial Maximum (LGM), it attained a similar extent to the present-day Antarctic Ice Sheet, providing an ideal location to study the behaviour of palaeo-ice streams.

The LIS reached its all-time maximum extent at the global LGM when the western margin coalesced with the CIS for the first time in the Quaternary, creating an ice saddle between the two ice sheets (Levson and Rutter, 1996; Jackson et al., 1997;
45 Bednarski and Smith, 2007). Most ice sheets had reached their maximum between 26.5 ka and 19 ka, although there are significant regional variations in the timing ice sheet sectors reached their maximum and here we use the term ‘LGM’ to refer to the local maximum extent of the northwestern sector at ~17.5 ka (Clark et al., 2009; Dalton et al., 2023). Numerical modelling indicates that abrupt climate warming during the Bølling-Allerød interval led to the expansion of the ablation area. This resulted in a mass balance-elevation feedback and rapid surface lowering in the ice saddle area, which is hypothesized to
50 have caused rapid global mean sea level rise (Gregoire et al., 2012; Gomez et al., 2015; Gregoire et al., 2016). However, this scenario is subject to debate, with Pico et al. (2019) linking the demise of the ice saddle with the shut-down and retreat of the Amundsen Gulf Ice Stream between 13 ka and 11.5 ka and thereby suggesting that the loss of the ice saddle occurred during the cooler period of the Younger Dryas. Nevertheless, recently published chronological constraints from the Northwest Territories identify a period of rapid ice sheet thinning during the Bølling-Allerød interval (Stoker et al., 2022).

55 The rapid collapse of the Cordilleran-Laurentide ice saddle is likely to have had a dramatic impact on the ice drainage network and ice stream activity during the last deglaciation, but this has not yet been investigated in detail (Margold et al., 2015a, b, 2018). A review of ice stream activity of the LIS through the last deglaciation (Margold et al., 2015a, b; 2018) shows that there is clear evidence for major ice stream systems that drained the ice saddle and Keewatin Dome of the LIS during the last deglaciation (Figure 1) (Winsborrow et al., 2004; Kleman and Glasser, 2007; Brown et al., 2011, Brown, 2012). However, it
60 remains unclear whether these large ice stream systems operated synchronously over large distances, or time-transgressively, switching on and off, with their trajectories migrating through time (Brown, 2012; Margold et al., 2015b, 2018). To the south of the saddle, on the southern Interior Plains in Alberta and Saskatchewan, for example, the



65 **Figure 1:** The ice stream reconstruction of the northwestern Laurentide Ice Sheet from Margold et al. (2015b) and selected glacial geomorphology (eskers, moraines and lineations) from the Glacial Map of Canada (Prest, 1968; Fulton, 1995). In the inset figure, the North American Ice Sheet Complex extent at the local LGM (17.5 ka) is depicted from Dalton et al. (2023). The approximate location of ice domes and ice divides is based on Margold et al. (2018) (LIS = Laurentide Ice Sheet, CIS = Cordilleran Ice Sheet, K = Keewatin, Q-L = Québec-Labrador dome, and F-B = FoXe-Baffin dome).



70 geomorphological record presented by Norris et al. (2023) indicates that major shifts in ice flow were associated with rapid downwasting of the Cordilleran and Laurentide ice saddle (Norris et al., 2022), but similar evidence has yet to be identified in the Northwest Territories.

Recent advances in the resolution of remotely sensed data allow us to investigate large areas of the subglacial bed of former ice sheets in detail (Chandler et al., 2018). Dulfer et al. (2023) recently used the high-resolution (2 m) ArcticDEM to produce a detailed glacial landform map of the northwestern LIS. Here we use this map to resolve the ice flow dynamics across the northwestern sector of the ice sheet. We employ a flowset mapping approach (e.g. Clark 1993, 1997; Kleman et al., 1997, 2006; Hughes et al., 2014) to reconstruct complex ice flow geometries and the relative ice flow dynamics, together with the distribution of ice-marginal landforms to identify former ice margin positions during ice retreat. The optimal ice margin chronology from Dalton et al. (2023) provides a temporal framework for our reconstruction, which allows us to investigate the following questions:

- How did the ice stream drainage network evolve spatially and temporally?
- How did the lobation and thermal regime of the ice margin evolve through deglaciation?
- How did the coalescence and separation of the ice sheets affect the configuration, timing and dynamics of the ice drainage network?
- 85 - What controlled the activation and shut-down of ice streams of the northwestern LIS?

2 Regional glacial history

Despite the remote nature of the region, the northwestern LIS, which spans western Nunavut and the majority of the Northwest Territories in Canada, has a long glacial research history. Since the early 1970s, extensive field surveys and aerial image mapping campaigns undertaken by the Geological Survey of Canada have detailed the surficial geology across the majority of the former bed of this ice sheet sector (Hughes and Hodgson, 1972; Hughes, 1987; Rutter et al., 1993). This mapping has been at a range of scales, from detailed 1:50,000 maps (e.g. Bednarski, 2002, 2003a-o) to coarser scale 1:1,000,000 compilation maps (e.g. Duk-Rodkin, 1999; Duk-Rodkin, 2022) and the majority of the work has been conducted at the relatively coarse 1:125,000 scale (e.g. Klassen, 1971; Rutter et al., 1980; Paulen and Smith, 2022). Recent projects have sought to deliver more comprehensive coverage or to improve upon the existing mapping (e.g. Smith et al., 2021; Hagedorn et al., 2022; Paulen and Smith, 2022). These studies have contributed to a detailed understanding of the former ice sheet limits and retreat pattern across the region, although it remains understudied compared to many other sectors of the former ice sheet (Rampton, 1988; Margold et al., 2018; Duk-Rodkin, 2022).

Our understanding of the northwestern LIS prior to the LGM is limited by the patchy record of older glaciations. Based on remote sensing evidence, Kleman et al. (2010) identified only a single westerly-directed ice flow event, which they correlated to Marine Isotope Stage (MIS) 4. In the central Keewatin region, a series of six till units from drillcore logs record a counter-

clockwise shift in the orientation of the Keewatin Ice Divide (Hodder et al., 2016). The single point nature of these subsurface observations makes it difficult to extrapolate over a larger area or to correlate with former ice margin positions. Evans et al. (2021) integrated sedimentological investigations, geomorphological mapping and cosmogenic nuclide burial dating to reconstruct a detailed glacial history of the Smoking Hills area (Figure 1). This invoked a significant revision of the glacial history of the region, with the concept of an early local glaciation of the Horton Plain by the Horton Ice Cap being rejected in favour of continental glaciation of the region at 2.9 ± 0.3 Ma and previous notions of multiple glaciations being replaced by a model of complex glacial sequences relating entirely to the Late Wisconsinan. These studies demonstrate that the northwestern LIS was characterized by complex dynamics during the last glacial cycle and the potential for multiple glaciations taking place throughout the Quaternary (cf. Batchelor et al., 2019) but details on the configuration and maximum extent of early glaciations in the region remain poorly constrained.

The configuration of the northwestern LIS since the local LGM is comparatively much better understood. The maximum extent is well established along the eastern range front of the Mackenzie and Richardson mountains (Hughes, 1972, 1987; Duk-Rodkin, 1999, 2022). In the Mackenzie Delta region, early reconstructions suggested that the ice sheet did not extend offshore and placed the LGM extent at moraines related to the Sitidgi Stade (Rampton, 1982, 1988). However, offshore geophysical surveys have revealed at least two, undated, advances to the shelf break, the most recent of which has been proposed to relate to the last glaciation (Batchelor et al., 2013, 2014; Riedel et al., 2021). Consequently, the Sitidgi Stade has been reinterpreted as a deglacial ice-margin position (Dalton et al., 2023) as part of a series of well-established deglacial limits (e.g. the Tutsieta and Kelly Lake phases defined by Hughes, 1987).

The advance and retreat of the northwestern LIS led to significant reorganisations of the drainage network and formation of glacial lakes (Smith, 1992; Lemmen et al., 1994; Smith, 1994; Dyke, 2004). As the LIS reached its maximum position along the northern Canadian Cordillera, it dammed the predominantly easterly-flowing fluvial drainage and formed a series of small lakes in the valleys of the Mackenzie Mountains (Duk-Rodkin and Hughes, 1991; Lemmen et al., 1994). In the northernmost region, in the unglaciated areas of the Yukon and beyond the Richardson Mountains, this resulted in the formation of Glacial Lake Old Crow, which has been used to constrain the timing of LIS advance to the local LGM (Lemmen et al., 1994; Zazula et al., 2004; Kennedy et al., 2010). In the early stages of deglaciation, glacial lakes Nahanni and Liard formed near the Liard Range, dammed by the LIS margin following its separation from the CIS (Bednarski, 2008). Continued deglaciation exposed a series of topographic basins formed by glacial isostatic depression and resulted in the formation of proglacial lakes along the ice sheet margin (Lemmen et al., 1994). This includes glacial lakes Mackenzie and McConnell, which coalesced with Glacial Lake Peace during their maximum stage to form one of the largest Pleistocene glacial lakes in North America (Smith, 1992, 1994; Lemmen et al., 1994). Although the evolution of these lakes has been reconstructed (Lemmen et al., 1994; Dyke, 2004), their influence on the dynamics and retreat of the northwestern LIS are less well known.

The sparse chronological constraints across the region led to conflicting reconstructions of the timing of deglaciation. Radiocarbon dating has been used to suggest an early local LGM extent at ~ 30 ka in this sector, with a significant readvance at ~ 22 ka (Duk-Rodkin et al., 1996, 2004; Zazula et al., 2004) and a phase of rapid retreat during the Younger Dryas Stade



135 (Dyke, 2004). The use of luminescence and cosmogenic dating methods, alongside a re-evaluation of the existing radiocarbon constraints using modern standards, indicate a much later advance at ~20ka to a short-lived local LGM (Kennedy et al., 2010; Murton et al., 2015) with deglaciation beginning at around 18-17ka (Stoker et al., 2022). In this new chronological model, a period of rapid retreat occurred during the Bølling–Allerød interval, with a period of stabilisation of the ice sheet margin on the Canadian Shield occurred during the Younger Dryas Stade (Reyes et al., 2022; Stoker et al., 2022; Dalton et al., 2023).

140 Our understanding of the ice flow dynamics of the northwestern LIS suffers from the disconnected nature of studies at varying scales. During the 1990s, the methodology for reconstructing ice flow dynamics using remote sensing data was established and provided fundamental insights into ice sheet drainage network through investigations of the entire LIS bed (Boulton and Clark, 1990; Clark, 1997; Kleman and Glasser, 2007; Kleman et al., 2010). However, this work did not result in a detailed reconstruction of the ice flow dynamics of the northwestern ice sheet sector, as it did with other sectors (e.g. Clark et al., 2000;

145 De Angelis and Kleman, 2005, 2007; Stokes et al., 2009). Regional scale studies have provided detailed ice flow reconstructions for some regions (e.g. Bednarski, 2008; Evans et al., 2021), but have limited coverage elsewhere. In particular, the Amundsen Gulf Ice Stream has been the subject of multiple studies both onshore and offshore (Stokes et al., 2006; Kleman and Glasser, 2007; Stokes et al., 2009; Batchelor et al., 2014), while the Mackenzie Valley region has received comparatively little attention since Beget (1987). The glacial geomorphological map of Brown et al. (2011), which covered the entire ice

150 sheet sector, was limited by the resolution of the available datasets at that time (Brown, 2012). The ice sheet wide reconstruction of ice stream activity by Margold et al. (2018) integrated the observations from these studies across the whole ice sheet but highlighted large uncertainties in the northwestern sector relating to the influence of the ice saddle on ice flow dynamics.

Recent regional-scale investigations have led to a reinterpretation of the ice flow dynamics of the northwestern LIS. In the

155 Smoking Hills-Horton River area, field observations of glacial stratigraphy and broader-scale geomorphological mapping have highlighted the nature of complex decoupling of ice margins relating to ice flow units derived from the south, east and southwest, with moraine belts recording the establishment of polythermal, debris-charged snouts during overall recession (Evans et al., 2021). South of Great Slave Lake, the formation of the Cameron Hills ice stream fragment had been tentatively interpreted as a deglacial flowset by Margold et al. (2018) but the till characteristics and fragmented nature of this flowset have

160 led to a reinterpretation that implies a much earlier formation when the Cordilleran and LIS merged (Hagedorn, 2022). Till fabrics at Pine Point, on the southern shore of Great Slave Lake, provide evidence for early ice flow to the SW across this region (Sapera, 2023). The coalescence of the LIS and CIS resulted in the NW ice flow during the local LGM, until separation of the ice sheets led to the re-establishment of ice flow to the WSW during deglaciation (Sapera, 2023). These studies provide a detailed record of relatively local glacial histories and have significantly improved our understanding of the regional ice flow

165 dynamics generally but are ultimately limited in extent. This means that large uncertainties still exist in our understanding of the changes in the ice drainage network at the ice sheet sector scale.



3 Methods

Our reconstruction is based on the glacial landform map of the northwestern sector of the LIS by Dulfer et al. (2023) which followed a uniform mapping approach across the entire region and was verified against surficial geological maps. This recent mapping facilitates a consistent ice flow reconstruction across the entire study area at relatively high-resolution, albeit with some inherent limitations (discussed in Section 3.4). The map contains twelve landform categories, including ice flow parallel lineations, subglacial ribs, crevasse fill ridges (geometric ridge networks), major and minor moraine crests, hummocky terrain complexes and ridges, shear margin moraines, major and minor meltwater channels, lateral and submarginal meltwater channels, esker ridges and complexes, glaciofluvial complexes, perched deltas, raised shorelines and aeolian dunes. Here we use the spatial distribution and characteristics of these glacial landforms to determine how ice flow and the related ice margins evolved over time, as outlined below.

3.1 Flowset mapping

We use the ~76,000 ice flow parallel lineations mapped by Dulfer et al. (2023) to decipher ice flow variation over time following the established approach of glacial flowset mapping (e.g. Clark 1993, 1997; Kleman et al., 1997, 2006; Greenwood and Clark, 2009; Hughes et al., 2014). We first reduced the amount of lineation data by drawing generalized ice flow lines parallel to the lineations and then used these flowlines to group coherent patterns of lineations into discrete flowsets (Kleman and Borgström, 1996; Kleman et al., 2006; Figure 2). We acknowledge that this process is subjective and some flowsets may have formed time-transgressively, but the different flow phases could not be distinguished in the landform record. Each flowset was assigned a number and the characteristics of the flowset were recorded, including the morphology of the flowset, the ice flow direction, the location of cross-cutting lineations and associated glacial landforms (see Supplementary Table 1). During the creation of the final flowset reconstruction, some flowsets were deleted, merged or split, leading to some flowset numbers being absent from the final map (e.g. Fs 210, 211, 264).

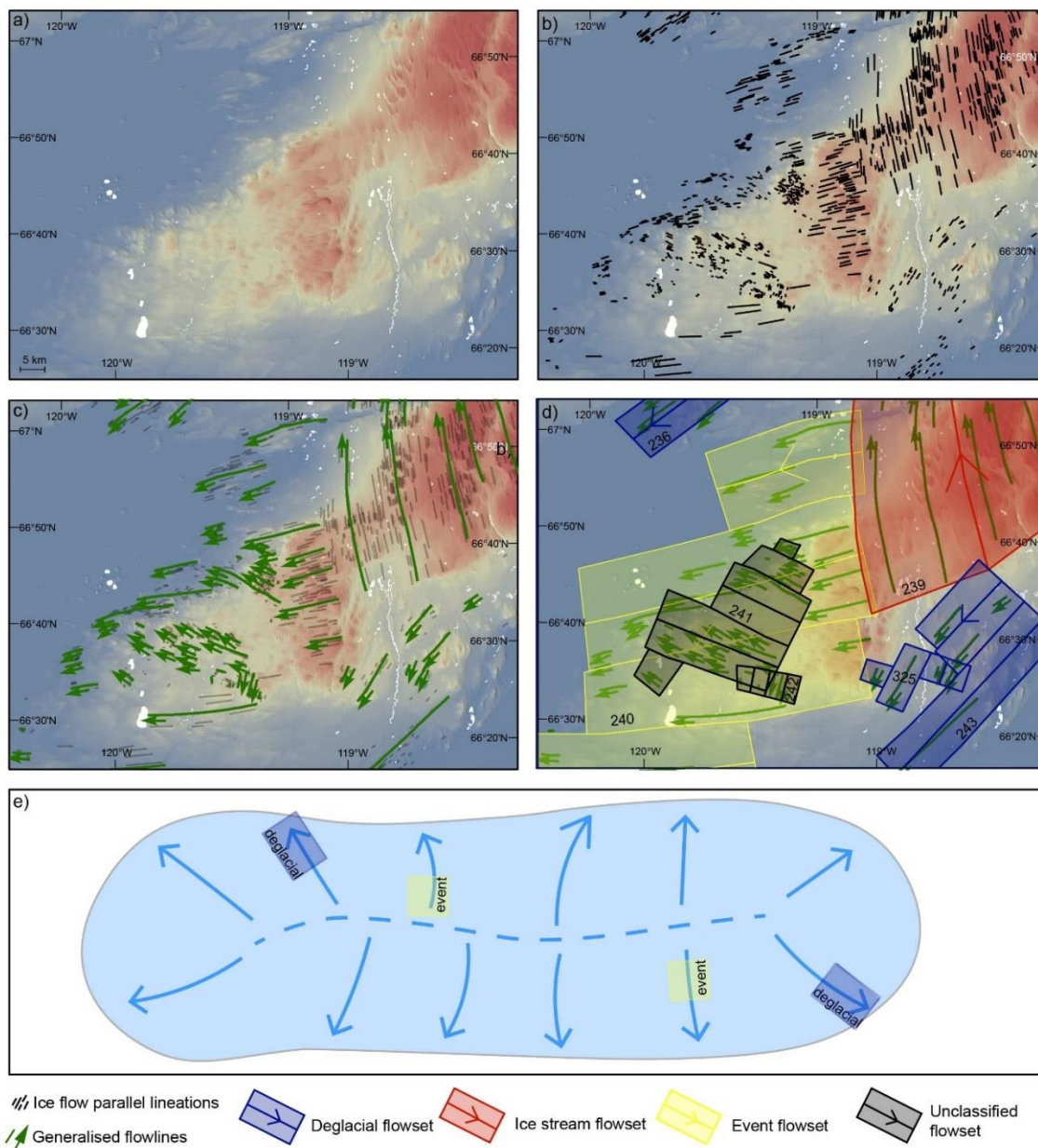
Flowsets were classified into one of the following categories based on cross-cutting relationships and an assessment of the diagnostic criteria listed in Table 1: ice stream, deglacial, inferred deglacial and event flowsets (see also Figure 2). The ice stream flowset category represents areas of past fast ice flow and are principally defined based on the elongation and parallel conformity of lineations, and the abrupt lateral edge of the flowset (Clark, 1993, 1999; Stokes and Clark, 1999). Ice stream flowsets can form in any position within an ice sheet, either near to the margin or towards the interior (Table 1, Figure 2e). In contrast, event and deglacial flowsets formed under a slower ice flow regime (Table 1) and are defined based on their location of formation within the ice sheet (Figure 2e). Deglacial flowsets formed near to the ice sheet margin and are identified based on their association with other deglacial landforms (e.g. eskers or moraines, Table 1). Inferred deglacial flowsets are suggested to have formed near the ice sheet margin but are not associated with deglacial landforms. Rather, ice-marginal formation is based on fan-shaped lineation patterns or a clear topographic influence on lineations (Table 1). Event flowsets are inferred to have formed within the interior of the ice sheet and are identified based on the absence of, or discordance with, deglacial



landforms and the high parallel conformity of lineations and their often fragmented nature (Table 1). Where there was insufficient information to classify the flowset, it was labelled as unclassified and not used in our reconstruction.

Table 1: Diagnostic criteria for flowset classification (modified from Kleman and Borgström, 1996; Stokes and Clark, 1999; Kleman et al., 2006; Greenwood and Clark, 2009; Hughes et al., 2014).

| Flowset type | Characteristics | Timing of formation within the flowset | Spatial classification/position in ice mass |
|---------------------------|---|--|---|
| Ice stream | <ul style="list-style-type: none"> - Highly attenuated bedforms. - Highly convergent flow patterns. - Abrupt lateral margins. - Lateral shear margin moraines. - Dispersal trains. - Lineations may be overprinted. | Synchronous or time transgressive | Ice marginal or interior |
| Deglacial | <ul style="list-style-type: none"> - Lineations aligned with eskers - Lineations associated with ice contact landforms, such as moraines. - Lineations influenced by topography. - No overprinting landforms. | Synchronous or time transgressive | Ice marginal |
| Inferred deglacial | <ul style="list-style-type: none"> - Lineations influenced by topography. - No overprinting landforms. - Fan-shaped lineation pattern | Synchronous or time transgressive | Ice marginal |
| Event | <ul style="list-style-type: none"> - High parallel conformity. - Lineations without meltwater landforms (e.g. eskers). - No association with moraines. - Abrupt lateral margins. - Lineations may be overprinted. | Synchronous | Interior |



210 **Figure 2: Example of the glacial flowset mapping methodology.** (A) ArcticDEM-derived hillshade imagery (Porter et al., 2018), (B) ice flow parallel lineations from Dulfer et al. (2023), (C) generalisation of the lineation data (green) with the ice flow parallel lineations underneath (black), (D) grouping coherent patterns of lineations into discrete flowsets with the generalised lineation data underneath (green). See Table 1 for the diagnostic criteria for classifying the flowsets. Arrows show the ice flow direction where it could be determined and the flowset numbers correspond to the numbers listed in Supplementary Table 1. Note the inferred deglacial flowset category is missing from this example.



215 **The location of this figure is shown on Figure 1. (E) Hypothetical ice sheet showing where the deglacial and event flowsets are formed within the ice body. Ice stream flowsets may form in either an ‘event’ or ‘deglacial’ position. The dashed blue line represents the ice divide, and the blue arrows show ice flow direction.**

3.2 Deglacial dynamics

220 The retreat pattern of the northwestern LIS is defined by a range of deglacial landforms, including moraines, hummocky terrain, eskers and lateral meltwater channels (Dulfer et al., 2023). Here we use this landform record to delineate past ice margin positions and inferred ice margin positions across our study area (Figure 3; Table 2) following protocols employed by Greenwood et al. (2007) and Clark et al. (2012, 2022). The inferred ice margins are necessarily subjective because they typically include extrapolation between geomorphological evidence. In some places this may be the extrapolation from a moraine or meltwater channels to depict an ice lobe based on glaciological process-form relationships and the influence of local topography. Additionally, we mark the former ice flow direction associated with each ice margin wherever it could be
225 determined using the glacial landform record. While glacial lakes are known to have formed along the retreating margin of the northwest LIS, we do not reconstruct glacial lakes here. Instead, we use the broad-scale reconstruction of lakes in Dyke et al. (2003) to make preliminary comparisons between ice stream activity and the location of large proglacial lakes.

3.3 Temporal framework

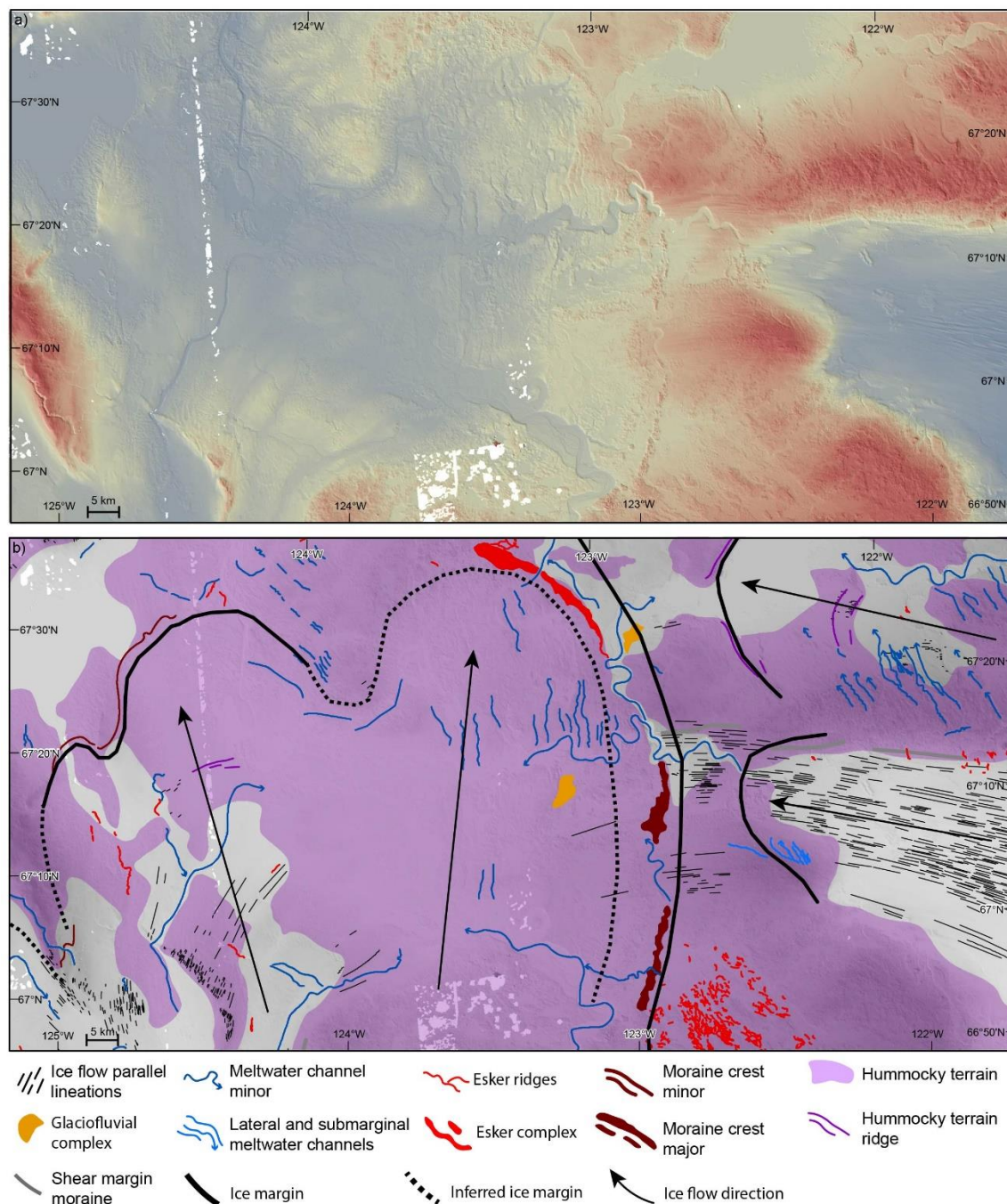
230 We use the ‘optimal’ ice margins from NADI-1 as a temporal framework for our reconstruction (Dalton et al., 2023). NADI-1 consists of isochrones of the entire North American Ice Sheet Complex from 25 ka to present in 500-year intervals based on all available geochronological constraints. Our geomorphology-based ice margin positions (see section 3.2) add considerable detail to the margin retreat pattern when compared with NADI-1. This is because they are not based on 500-year timesteps and so better capture the detail of the ice retreat and separation of multiple ice lobes in between the regular 500-year time-steps. However, as most of the geomorphology-based ice margins are not directly dated, it is not possible to provide a more detailed
235 chronological placement for them beyond the temporal framework of NADI-1 (Dalton et al., 2023). In summary, we do not adjust the ice margin outline of the NADI-1 isochrones, as to do so would require a re-examination of the chronological constraints on deglaciation, which is beyond the scope of this paper (cf. Dalton et al., 2023). Instead, we provide our geomorphology-based ice margins as a supplement to this temporal framework to aid in the understanding of ice flow evolution changes.

240



Table 2: Description of ice marginal landforms used to map former ice marginal positions during the last deglaciation.

| Landform | Description | Ice marginal position | Reference |
|---------------------------|---|---|--|
| Terminal moraine | Sharp-crested straight or arcuate-shaped ridges of sediment. | Form by deposition or deformation of glaciogenic sediment along active ice margins. | Benn and Evans (2010) |
| Lateral meltwater channel | A series of parallel or subparallel channels that all dip in the same direction. Often occur as a series of channels perched on valley sides. | Form by water flowing along the ice margin. Sequences of lateral meltwater channels can delineate ice sheet surface lowering and ice marginal retreat through time. | Mannerfelt, (1949), Greenwood et al. (2007, 2016). |
| Hummocky Terrain | Irregular surface containing mounds of sediment alternating with depressions. | Form at a stagnating ice margin by a combination of processes. | Evans et al. (2021) |
| Esker | Sinuuous depositional ridges of glaciofluvial sand and gravel. | Deposited by meltwater flowing through, beneath or above ice. Eskers form time-transgressively normal to the ice margin. | Shreve (1985), Hebrand and Åmark (1989), Storrar et al. (2014a). |



245 **Figure 3: Delineating former ice margin positions from the glacial landform record. (A) ArcticDEM-derived hillshade imagery (Porter et al., 2018) and (B) glacial geomorphological mapping from Dulfer et al. (2023). The ice contact landforms, including major and minor moraines, hummocky terrain ridges, eskers and lateral and submarginal meltwater channels, have been used to draw the ice margin and inferred ice margin positions, which are shown by the black solid and dashed lines, respectively. The ice flow direction is shown by the black arrows. This is an example of**



250 **interlobate ice margins. Note how the main deglacial landforms (moraines and hummocky terrain) are overprinted on the westwards ice flow signature. The location of this figure is shown on Figure 1.**

3.4 Limitations and uncertainties

The reconstruction of Late Quaternary glaciations from remote sensing data is a low-cost and relatively time-efficient method for covering large areas, but also includes fundamental limitations irrespective of the used data resolution (Chandler et al., 255 2018). In this study, we reconstruct the ice flow evolution of the northwestern LIS based on the glacial geomorphological map of Dulfer et al (2023). This map is composed solely of glacial landforms visible at the earth surface from the ArcticDEM (2 m resolution; Porter et al., 2018). Despite the high-resolution of these data, the landform record has clear limitations when trying to reconstruct the glacial history in areas with complex, changing flow patterns or a history of multiple cycles of glaciation. The most recent glaciation often erodes and reworks the existing surficial record, meaning that the surface geomorphology is 260 only a snapshot of the last landform-creating glacial event over a region and not a composite of the entire glacial history. The last glaciation represents the all-time maximum extent of the northwestern LIS, so there is limited geomorphological evidence of older glaciations at the surface. The subsurface record may retain a signal of earlier glaciations and can often be used to reconstruct the longer-term history or better constrain the relative sequence of flow events (Hodder et al., 2016). Multiple studies (e.g. Bednarski, 2008; Stokes et al., 2006; Evans et al., 2021), alongside surficial geological mapping campaigns by 265 the Geological Survey of Canada (e.g. Hagedorn et al., 2022; Smith et al., 2022), provide more detailed, but more narrowly-focused reconstructions of the glacial history. Glacial striations also provide an opportunity for reconstructing former ice flow patterns and may preserve older flow traces on bedrock outcrops where abrasion was limited during deglaciation (Kleman, 1990). The key advantage of our reconstruction is that we reconstruct the ice flow dynamics at the ice sheet sector scale to gain an insight into the LIS evolution during deglaciation.

270 The isochrones of Dalton et al. (2023) for the northwestern LIS are largely anchored by cosmogenic nuclide exposure ages. Cosmogenic nuclide exposure dating includes uncertainties of up to 10% (Stoker et al., 2022) of the measured age, meaning uncertainties can exceed 1,000 years for samples from the LGM (Stoker et al., 2022). As there is no universal method for calculating exposure ages, a range of different calibration data, scaling schemes and correction factors may be applied and the chosen approach can lead to calculated exposure ages that differ by over 1,000 years (Stoker et al., 2022; Reyes et al., 2022). 275 However, the rates of retreat are typically consistent between exposure age calculation approaches, and it is the timing of deglaciation that is shifted. As our ice flow reconstruction is constrained by cosmogenic nuclide exposure ages it is subject to change due to advances in our understanding of cosmogenic nuclide exposure age dating.



4 Results

4.1 Ice flow reconstruction

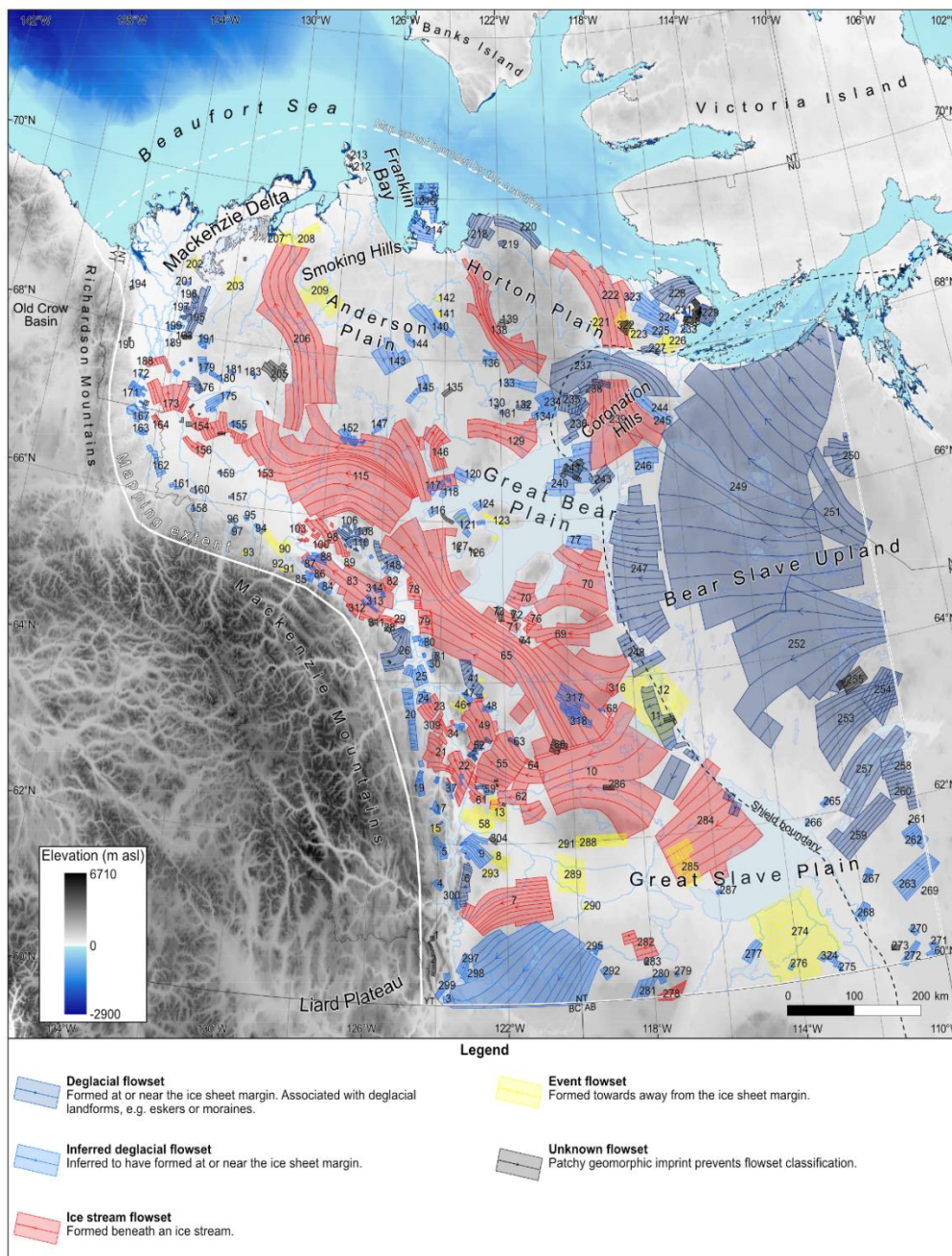
280 We identified 326 flowsets across the bed of the northwestern LIS (Figure 4; see Supplementary Figure 1 for A0 version where all flowsets are labelled). This includes 62 deglacial, 133 inferred deglacial, 53 ice stream, 33 event, and 46 unclassified flowsets. These flowsets range in size from a few km² to over 80,000 km² (e.g. Fs-249). The 2 m resolution of the ArcticDEM allowed us to classify lineations into separate flow events in greater detail than the previous broad-scale work (e.g. Margold et al., 2018). In this section, we provide a broad overview of our flowset map (Figure 4). A detailed description of individual
285 flowsets can be found in Supplementary Table 1 and all shapefiles are available in Supplementary Folder 1. We then place this ice flow evolution into a temporal framework in Section 5.

4.1.1 Ice stream flowsets

Ice stream flowsets are composed of highly attenuated subglacial bedforms, including elongate drumlins and mega scale glacial lineations (MSGL). They exhibit a wide range of sizes, from small flowset fragments (~15 km²) to large flowsets up to 40,000
290 km². The geometry of the larger flowsets is varied, with converging (e.g. Fs 10, 129, 239, 284), diverging (e.g. Fs 55, 62, 154, 173) and hourglass-shaped (e.g. Fs 65, 70, 115, 138, 206) lineation patterns. Ice stream flowsets are observed across the entirety of the Northern Interior Plains region in the west but are absent from the Canadian Shield region in the east (Figure 4). The dominant orientation of ice flow from ice stream flowsets is to the north and the northwest ($n=38$). There are also multiple ice stream flowsets indicating ice flow to the west ($n=15$). In general, the westerly-oriented ice stream flowsets are superimposed
295 on, or cross-cut, the northerly-oriented flowsets.

4.1.2 Deglacial flowsets

Deglacial flowsets are the second-most prevalent flowset type and are observed across the whole region (Figure 4). The lineations in this flowset-type are generally well preserved and not overprinted by other landforms. However, the northerly-oriented deglacial flowsets tend to be overprinted by westerly-oriented deglacial flowsets. The complexity of these overprinting
300 patterns is described in Section 5. They exhibit the largest range in flowset size. The smallest flowset is ~5 km² and the largest is just over 80,000 km². There are two main flowset geometries: a lobate flowset pattern of diverging lineations and a flowset geometry composed of parallel lineations. The lineation pattern in these flowsets is often influenced by the local topography. On the Northern Interior Plains, the deglacial flowsets are predominantly composed of drumlins, which can be parallel or diverging in a lobate pattern. These flowsets display a range of orientations. In the foothills of the Mackenzie Mountains, their
305 orientation is strongly influenced by the local topography. In some places this topographic control results in adjacent flowsets with opposing flow directions as the thinner ice sheet during deglaciation means that the topographic gradient rather than the ice surface slope becomes the dominant control on ice flow direction.



310 **Figure 4: Flowset map of the northwest sector of the Laurentide Ice Sheet. Flowsets have been assigned a number with corresponding information available in Supplementary Table 1. Due to the scale of the figure, only the largest flowsets are labelled in this figure. An A0 version of this map is provided in the supplementary materials, which includes labels for each flowset and information on the cross-cutting of different flowsets (Supplementary Figure 1). The flowsets are classified according to the criteria in Table 1.**



315 On the Canadian Shield, crag-and-tails and streamlined bedrock are the dominant lineation type although some pre-crag features are also observed. These lineations are generally shorter than those observed on the Northern Interior Plains. Flowsets on the Canadian Shield tend to form a large, diverging flow pattern of subparallel lineations that are broadly oriented towards the west. There is overprinting of the large diverging flow pattern (Fs 249, 252) by smaller flowsets, which appear to be influenced by the local topography.

320 **4.1.3 Inferred deglacial flowsets**

Inferred deglacial flowsets are the most common flowset type across the study region. Most of the flowsets in this category are small, with only one flowset exceeding 3,500 km² in area. Unlike deglacial flowsets, these flowsets are not directly associated with any deglacial landforms. However, they commonly exhibit a lobate geometry or display deflections around the local topography, which is indicative of a thinner ice sheet and formation near the ice sheet margin (Kleman and Hättestrand, 1999; Kleman et al., 1999; Hughes et al., 2014). The geomorphic imprint of these flowsets typically displays well-preserved lineations that are not overprinted by other landforms. These flowsets are more commonly found at lower elevations, along the valley floors, and are rarely located on summits, ridgelines or elevated plateaus. South of 62°N, these flowsets are broadly oriented towards the southwest. North of 62°N, the dominant orientation is towards the west or northwest. Similar to the deglacial flowsets, there is a strong topographic influence on flowset orientation which results in local-scale complexity.

325
330 In the central Mackenzie Valley, between 63°N and 66°N, this influence is clear, with multiple flowsets oriented towards the south (Fs 24, 25, 27, 30, 31, 32, 33, 47, 80), i.e. up-valley, against the direction of flow indicated by adjacent flowsets in the Mackenzie Valley to the north and south. Towards the Canadian Shield, in the east, ice flow is oriented more broadly towards the west.

4.1.4 Event flowsets

335 Event flowsets are the least common flowset and are composed of short drumlins and streamlined bedrock. Lineations display a high parallel conformity regardless of the local topographic factors. Where these flowsets are located at lower elevations they are often overprinted by other flowsets (e.g. Fs 12, 274, 285) and at higher elevations they are typically well-preserved, with little overprinting (e.g. Fs 48, 288). The majority of event flowsets are smaller than 1,000 km², but they can be up to 11,000 km². There is no dominant orientation of event flowsets which likely indicates these flowsets are formed over different events and times of glaciation.

340

4.1.5 Unclassified flowsets

Unclassified flowsets are quite rare across the study area (n = 46) and are generally composed of poorly preserved lineations with a patchy geomorphic signature. These flowsets are often overprinted by other glacial landforms or disturbed by postglacial processes. They are mostly small (less than 30 km²) and with no clear preferred orientation. A small number of the unclassified



345 flowsets have a clear geomorphic signature, but the absence of any relationship with other flowsets or landforms make them difficult to classify or place in a relative time sequence (Fs 1, 2).

4.1.6 Comparison of flowsets with previous broad-scale work

The ice flow patterns of the northwestern LIS have been reconstructed at various scales in previous work. This includes multiple broad-scale reconstructions that cover the entire study area (Kleman et al., 2010; Shaw et al., 2010; Margold et al., 350 2015a, b, 2018) and one unpublished flowset reconstruction by Brown (2012), which covers almost the entire area of this study. Our flowsets were mapped independently of previous work, but we note whether each flowset has been previously mapped in Supplementary Table 1.

Margold et al. (2015a, b, 2018) mapped past ice stream activity at the ice sheet scale and their mapping matches 64% of our mapped ice stream flowsets (based on the number of our ice stream flowsets that are located within those of Margold et al. 355 (2015a, b, 2018)). Our reconstruction provides some additional detail compared to that of Margold et al. (2015a, b, 2018). Firstly, our reconstruction attempts to capture all past ice flow events in the landform record and not simply the fast ice flow signature. Secondly, our reconstruction is at a higher resolution, which can provide greater detail for reconstructing past ice stream activity.

The flowsets of Kleman et al. (2010) match 37% of the flowsets in our reconstruction. Only 26% of the flowlines mapped by 360 Shaw et al. (2010) match our flowsets, and these flowlines are not categorized into flowsets. The reconstruction of Brown (2012) only extends to 115° W, while our reconstruction extends to 110° W, but in the shared map area, Brown (2012) identified ~45% of the flowsets in our reconstruction. In general, this is the result of the high-resolution ArcticDEM allowing the identification of small flowsets that were beyond the resolution of these previous studies and for categorizing previously mapped flowsets with much higher confidence.

365 Our flowset map broadly matches the existing ice flow reconstructions that have been undertaken at a more local scale, but often contains less detail. In the region surrounding the Amundsen Gulf Ice Stream (Fig. 1), which has figured in previous ice flow reconstructions (e.g. Stokes et al., 2006, 2009), our flowset map captures previously described flow events but the flowsets often have a different geometry, as they have been drawn based on different datasets. In this region, our flowset map is also limited by the lack of offshore data in our reconstruction, so does not attempt to reconstruct or copy these flow events across 370 from previous studies. In the Smoking Hills region (Figure 1), the flowset map of Evans et al. (2021) exceeds the detail presented in our map and hence a few small (<400km²) flowsets are not depicted in our reconstruction. Just east of the Liard Plateau (Fig. 1), Bednarski (2008) reconstructed the ice flow patterns and glacial lake history during deglaciation. While this reconstruction does not present a formalized flowset map, the ice flow patterns presented match well with our flowset map.

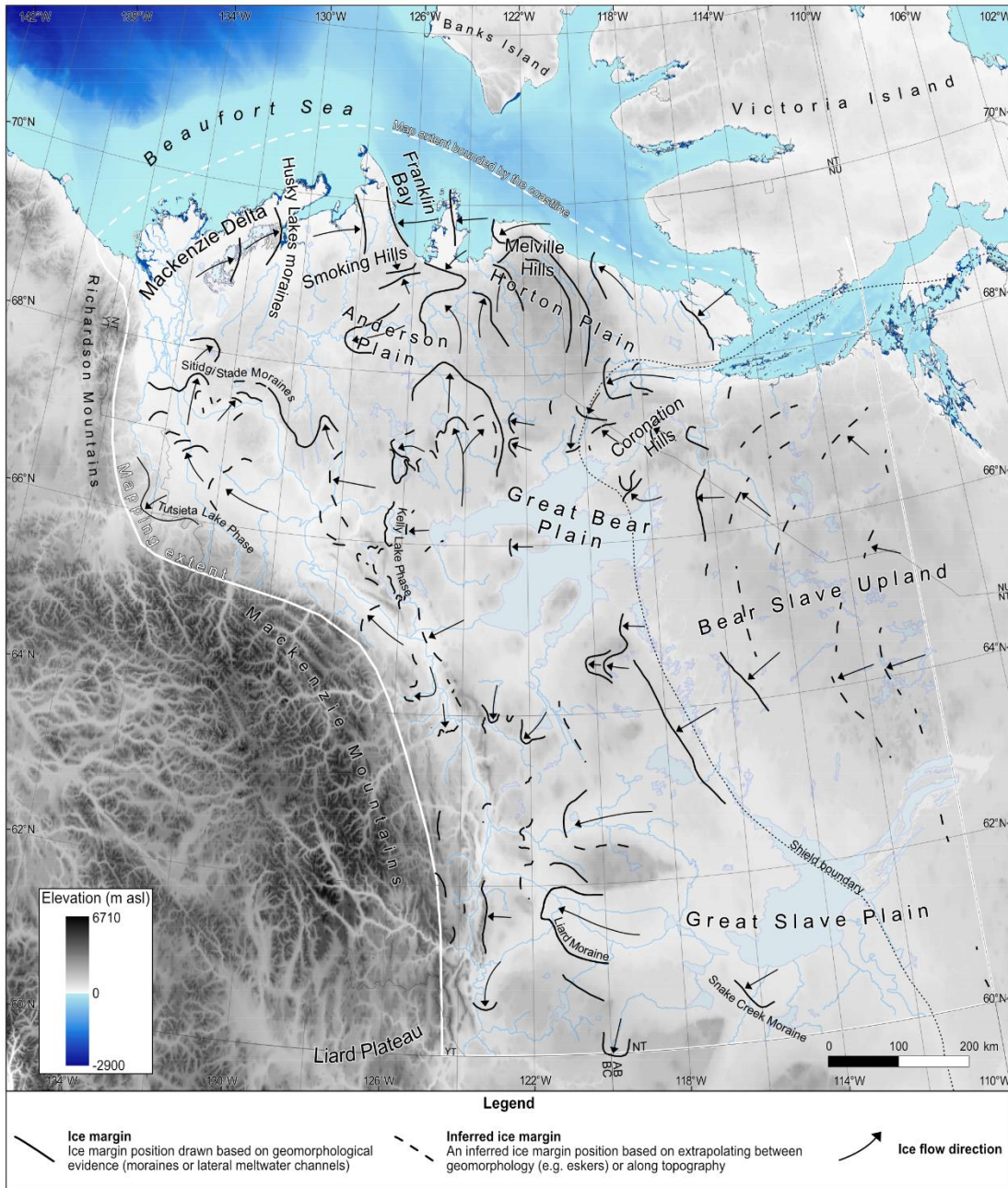
4.2 Ice margin retreat record

375 Ice-contact landforms have been used to mark deglacial ice margin positions and associated ice flow directions across the study area (Figure 5). In the northwest, hummocky (controlled) moraine belts are the dominant ice-contact deglacial landform



(Evans et al., 2021), but former ice margin positions in this region are also delineated by end moraines and lateral/submarginal meltwater channels. On the Canadian Shield to the east, these landforms become much less common and the deglacial retreat pattern is recorded by eskers. Here the ice margin is extrapolated between eskers based on the assumption that eskers form
380 time-transgressively perpendicular and proximal to the ice margin (Shreve, 1985; Storrar et al. 2014a; Livingstone et al., 2015). Our record of deglacial ice margin positions shows a large variation in ice flow direction throughout deglaciation (Figure 5). In the north of the study area, two opposing ice retreat directions are mapped: (1) ice retreat to the west, marked by the Husky Lake Moraines; and (2) ice retreat towards Victoria Island in the east (Figure 5). On the Horton Plain and in the northern Mackenzie Valley, the ice-contact landforms were deposited as the ice margin retreated to the south and southeast respectively
385 (Figure 5). Over the eastern portion of the study area, including the Great Slave Plain and the Canadian Shield, the former ice margins record a general ice retreat pattern towards the east, with localised southerly ice flow around topographic features (Figure 5).

In the north, where opposing ice retreat patterns are mapped, the ice margin retreat pattern is complex due to the separation of different major ice lobes, with the landform record documenting several interlobate ice margins. The most notable example is
390 located in the Coronation Hills and is delineated by a prominent moraine and esker system. Deglacial interlobate ice configurations have also been previously identified during deglaciation of the LIS in the Smoking Hills region of our study area (Evans et al., 2021). We provide a simplified reconstruction of the ice margin retreat pattern in this region.



395 **Figure 5: The ice margin retreat pattern of the northwestern Laurentide Ice Sheet based on the deglacial landforms from Dulfer et al. (2023). We label the landforms that have previously been identified and used to establish the deglacial retreat pattern in the literature. This includes the Liard Moraine (Smith, 1994), Snake Creek Moraine (Lemmen et al., 1994), landforms of the Kelly Lake Phase and Tutsieta Lake Phase (Hughes, 1987), Sitidgi Stade moraines (Rampton, 1988), and Husky Lakes thrust moraines (Dyke and Evans, 2003; Evans et al., 2021). The ice margin retreat pattern in**



400 **the Smoking Hills area is simplified due to the scale of the map, for a more detailed ice margin reconstruction in this area see Evans et al. (2021).**

5 Interpretation

5.1 Overview of ice flow evolution through time

Prior to the local LGM, the northwestern LIS advanced westwards towards the Canadian Cordillera (Kleman and Glasser, 2007; Margold et al., 2018) (Figure 6a). The Amundsen Gulf Ice Stream was likely active during ice advance to the local LGM
405 extent and flowed into the eastern Beaufort Sea (Figure 6b; Stokes et al., 2006; Batchelor et al., 2014). However, there is limited geomorphological evidence of other ice streams being active at this time, which is likely because the evidence of ice advance has been overprinted by the deglacial signature or postglacial processes. The local LGM of the northwestern LIS occurred relatively late compared to the rest of the ice sheet (~17.5 ka, Dalton et al., 2023), following the coalescence of the LIS with the CIS and the formation of an ice saddle between the ice sheets. At this time, ice flow was directed predominantly
410 to the north or northwest across the study region. The ice flow network was drained by two major, marine-terminating ice streams, the Amundsen Gulf Ice Stream and the Mackenzie Trough Ice Stream, the former fed with ice from the Keewatin Ice Dome and the latter from the CIS-LIS ice saddle (Figure 6b; Batchelor et al., 2013, 2014; Margold et al., 2018).

Deglaciation of the northwestern LIS was characterized by periods of rapid retreat and thinning interspersed with periods of slow retreat (Reyes et al., 2022; Stoker et al., 2022; Dalton et al., 2023). The ice drainage and the ice stream network evolved
415 in response to these changes. The initial deglaciation of the northwestern LIS was characterized by slow ice margin retreat and a relatively stable ice drainage network (Dalton et al., 2023). The Amundsen Gulf Ice Stream was the main drainage outlet of the LIS in the eastern Beaufort Sea area and remained active throughout the early period of deglaciation, with minor reorganisations of the ice stream source area (Figure 6B-F; Stokes et al., 2006, 2009). The main drainage outlet in the western Beaufort Sea alternated between the Mackenzie Trough Ice Stream and the Anderson Ice Stream, which were likely not active
420 at the same time and were fed by the ice saddle between the CIS and LIS (Figure 6B-F).

The Bølling–Allerød interval (14.6 – 12.9 ka) was a millennial-scale warming event that occurred during the last deglaciation that is associated with rapid retreat of Northern Hemispheric ice sheets and glaciers (Lambeck et al., 2014; Menounos et al., 2017). Increasing temperatures during the Bølling–Allerød interval have been reconstructed to have triggered the collapse of the ice saddle between the CIS and LIS, which was followed by a period of rapid ice sheet thinning and retreat (Gomez et al.,
425 2015; Gregoire et al., 2016; Stoker et al., 2022). In response, the ice drainage network evolved rapidly, and the Keewatin Ice Dome became increasingly dominant as an ice source. This change in the relative dominance of ice source area is recorded in a shift from broadly northerly-oriented ice flow from the ice saddle to northwesterly flowing ice and finally westerly-oriented ice flow from the Keewatin Dome (Figure 6G-J). The ice stream network also adjusted rapidly to these changes. The loss of the ice saddle resulted in a limited contribution to the Amundsen Gulf Ice Stream directly from the mainland of Canada, with
430 ice for this ice stream coming from the Keewatin dome through Victoria Island (Figure 6G). The Paulatuk Ice Stream became



active in the area immediately west of the former Amundsen Gulf Ice Stream and its northwesterly-oriented flow direction reflects the increasing importance of the Keewatin Ice Dome (Figure 6H). In the northern Mackenzie Valley region, ice stream activity became dominated by westerly flow, as demonstrated by the activation of the Bear Lake Ice Stream (Figure 6G). Rapid retreat continued across the Northern Interior Plains following the separation of the CIS and LIS, with this period characterized
435 by westerly-oriented ice flow and relatively short-lived ice streams (Figure 6I and J).

The Bølling–Allerød interstadial was followed by the Younger Dryas Stadial (12.9 – 11.8 ka), which was a cool period that has been associated with glacier and ice sheet stabilization or advance (Lambeck et al., 2014), primarily in regions surrounding the North Atlantic (Rea et al., 2020; Mangerud, 2021). The beginning of the Younger Dryas coincides with a slowdown in the retreat rate of the northwestern LIS margin as it reached the Canadian Shield. This slow-down in ice retreat was accompanied
440 by a change in the ice flow dynamics (Figure 6K–P) from fast ice flow with numerous ice streams, which evolved rapidly through the deglaciation on the Northern Interior Plains, to a slower ice flow regime and a radial ice flow pattern fed by the Keewatin Ice Dome on the Canadian Shield. The exact control on this change in ice flow dynamics is unclear but is likely related to the switch from the soft-bedded, lake-terminating margin on the Northern Interior Plains to the hard-bedded, terrestrial margin on the Canadian Shield (see section 6.3 for a more detailed discussion).

In the following section, we describe in detail the changes in ice flow direction and dynamics at 500-year timesteps, constrained by the ice margin chronology of Dalton et al. (2023) (Figure 6). At various timesteps, we use our reconstructed ice margins (Figure 5) to provide further detail on the ice margin retreat pattern. The relatively coarse timestep of the ice margin chronology compared to our ice flow reconstruction means that conflicting flow directions may occur within a single timestep. In these situations, we define the distinct flow events as flow phases (whereby flow phase 1 represents an earlier flow event, which has
450 been overprinted by flow phase 2) and in Figure 6 we use different ice flow line styles to depict these separate flow phases.

5.2 Detailed reconstruction of ice flow

5.2.1 Pre-LGM flowsets

The signature of pre-LGM ice flow is sparse across the study area because the surficial geomorphological record typically only
455 records the most recent flow event (for more detail see section 3.4). Despite this, we assign multiple flowsets to the pre-LGM period (Figure 6A). Fs-240 (Figure 6A, mid-figure) is one of the oldest flowsets we identify and it represents early ice flow towards the west, as the LIS advanced over this region and before the initiation of the Amundsen Gulf Ice Stream. This pre-LGM westwards advance is well-established (Kleman and Glasser, 2007; Margold et al., 2018). The Amundsen Gulf Ice Stream operated as a major drainage outlet of the northwestern LIS throughout the Quaternary and likely operated prior to the
460 local LGM in this region (Batchelor et al., 2014). We interpret Fs-221, 223, and 226 (Figure 6A, top-right) as forming in the onset zone of an early Amundsen Gulf Ice Stream. In contrast, the Mackenzie Trough has a relatively short history of glaciation, with the offshore stratigraphic record suggesting only two previous Quaternary ice advances (Batchelor et al., 2013). The most



recent advance occurred during the last glaciation and likely contributed to the advance of the LIS to its maximum extent at the continental shelf break (Bateman and Murton, 2006; Batchelor et al., 2013). Flowsets 89, 98, 100, 103, and 104 all indicate
465 fast ice flow over undulating terrain with a deflection to the west (Figure 6a, mid-left). This deflection aligns the lineations within these flowsets with ice flow down the Mackenzie Valley. The lack of influence of the subglacial topography on these flowsets suggest that they did not form in an ice marginal location but were formed some distance up-ice (Siegert et al., 2004; Winsborrow et al., 2010; Hughes et al., 2014). Therefore, we interpret these lineations as forming in an up-ice area of the Mackenzie Trough Ice Stream. The exact timing of operation of these flowsets is difficult to identify, but they are cross-cut by
470 later multiple flowsets, suggesting they formed early during glaciation. Finally, we suggest that the Cameron Hills Fragment (Fs-278, bottom-centre) represents an early ice stream that operated as the LIS and CIS coalesced prior to the LGM, following the interpretation of Hagedorn (2022). The Cameron Hills Fragment is overprinted by other multiple flowsets and located at a high elevation, which supports the interpretation of formation during an early flow event (Hagedorn, 2022), as opposed to formation during deglaciation as proposed by Margold et al. (2018).

475 **5.2.2 From timeslice 17.5 to 17.0 ka**

The local LGM of the northwestern LIS was short-lived, reaching its maximum extent at 17.5 ka and subsequently retreating by 17.0 ka (Bateman and Murton, 2006; Kennedy et al., 2010; Dalton et al., 2023). During this period, the Amundsen Gulf Ice Stream operated in the eastern Beaufort Sea, fed by ice flow from the Keewatin Ice Dome (Fs-221, 223, and 226, top-right) and from Victoria Island (Stokes et al., 2006 and 2009; Batchelor et al., 2014). As the Amundsen Gulf Ice Stream advanced
480 to the west, it deflected ice flow across the Anderson Plain and Mackenzie Delta region to the west, as indicated by Fs-207 (Figure 6B, top-left). The Mackenzie Trough Ice Stream was also active at this time and deflected to the west. This westward deflection is necessary to form the thrust mass of Hershel Island (Dyke and Evans, 2003; Wetterich et al., 2023). Widespread fluvial reworking, periglacial processes and deglacial flow signatures in the Mackenzie Delta region mean that there is a limited signal of the Mackenzie Trough Ice Stream, with the clearest signature being observed further up-ice (Fs 89, 98, 100, 103, and
485 104, mid-left). It is likely that some of the unclassified flowsets (e.g. Fs 189, 190, 194, 204; Figure 6A, top-left) in this area were formed during the operation of the Mackenzie Trough Ice Stream but have been modified following deglaciation. The ice flow pattern at this time displays a clear orientation to the north and northwest, indicative of two main ice source areas: the Cordilleran-Laurentide ice saddle to the south and the Keewatin Ice Dome to the east.

5.2.3 From timeslice 16.5 to 16.0 ka

490 Between 16.5 ka and 16.0 ka, the Amundsen Gulf Ice Stream remained as the main outlet draining ice from the Keewatin Dome to the eastern Beaufort Sea (Figure 6D and E). During this time, there was a reorganisation of the ice stream network on the western Northern Interior Plains, as neighbouring ice streams switched off and on. On the Anderson Plain, highly attenuated and continuous lineations (Fs-206; Figure 6D and E, top-left) record fast ice flow as the Anderson Ice Stream

switched on and became the main drainage outlet from the Cordilleran-Laurentide ice saddle region to the western Beaufort
495 Sea.

The terminus of the Anderson Ice Stream (Fs-206; Figure 6D and E, top-left) is deflected to the east with no clear ice flow to
the west. This deflection has two important implications for the ice sheet configuration at this time: (1) the Amundsen Gulf
Ice Stream had retreated far enough to the east that it no longer provided a buttressing effect on ice flow across the Anderson
Plain; and (2) that ice was present in the adjacent Mackenzie Valley, restricting ice flow in this direction. The relatively late
500 activation of the Anderson Ice Stream following the retreat of the Amundsen Gulf Ice Stream is supported by an offshore
seismic sedimentary sequence presented by Batchelor et al. (2014), who show that the youngest till within the Amundsen Gulf
Trough was deposited by the Anderson Ice Stream.

Deglacial and event flowsets (Fs 195, 199, 200, 201, 202, 203; Figure 6E, top-left) provide evidence for a slower flow regime
in the Mackenzie Valley at this time and the shut-down of the Mackenzie Trough Ice Stream. The ice flow patterns and
505 deglacial landforms in the Mackenzie Valley between 68°N and 69°N record the slow retreat of an ice lobe up-valley. The
broad controlled moraine belts that were deposited during the Sitidgi Stade (Rampton, 1988) and a series of recessional, push
moraines record readvances of a debris-rich polythermal snout (Evans et al., 2021). Based on the change in ice flow regime in
the Mackenzie Valley, we suggest that the Mackenzie Trough Ice Stream and the Anderson Ice Stream were not active at the
same time, but alternated in activity during deglaciation, although the causes of the switch in ice stream routing are uncertain
510 but may relate to the proximity of Amundsen Gulf ice and the buttressing it provides.

5.2.4 From timeslice 15.5 to 15.0 ka

Deglaciation was relatively slow immediately prior to the start of the Bølling-Allerød interstadial (14.7-12.9 ka), with changes
in the ice drainage network resulting from the reorganisation of the active ice streams (Figure 6F and G). Two distinct flow
phases of the Amundsen Gulf Ice Stream can be identified from the cross-cutting flowset patterns in the Coronation Hills
515 region. The early flow phase (Fs 221, 223, 226; Figure 6B-E, top-right), depicted in previous timesteps, is broadly oriented
towards the northwest and sustained mostly by ice flow from the Keewatin Ice Dome in the east. The geomorphic record of
this early flow phase is fragmented and overprinted by later flow events, including Fs 222 and 239 (Figure 6F and G, top-
right), which also demonstrate a northerly ice flow components and indicate the growing influence of the ice saddle which fed
the Amundsen Gulf Ice Stream alongside the Keewatin Ice Dome. The exact timing of these flow phases is difficult to
520 determine but is constrained by two events. The later flow phase must have occurred at or after the LGM, as it is overprinted
on flowsets which formed during the LGM or pre-LGM period (Fs 221, 223, 226). The clear northwards orientation of this
flowset indicates ice flow from the saddle region, so this flow phase must have occurred before the collapse of the ice saddle
during the Bølling-Allerød interstadial (Stoker et al., 2022). The well-preserved nature of Fs 222 and 239 suggests that they
relate to the final phase of ice flow from mainland Canada, over the Coronation Hills, to the Amundsen Gulf Ice Stream.
525 Following the end of this flow phase, any fast ice flow in the Amundsen Gulf must have been sustained by ice principally
sourced from the Keewatin Ice Dome over southwestern Victoria Island and not the ice saddle. Therefore, we suggest that this



flow phase of the Amundsen Gulf Ice Stream likely occurred between 15.5 and 15.0 ka while the ice saddle remained thick enough to influence ice flow dynamics (Figure 6F).

The retreat of the LIS margin in the Northern Interior Plains led to changes in the ice flow regime. As the ice margin retreated up the Mackenzie Valley, the slower ice flow regime (Fs 191, 192, 195, 196, 197, 198, 199; Figure 6F and G, top-left) changed to a faster ice flow regime (Fs 154, 156, 164, 173, 188; Figure 6F and G, top-left) due to the reactivation of the Mackenzie Trough Ice Stream around 67°N. The lobate shape of the flow patterns (e.g. Fs 154, 173, 188) suggests that they were formed at the margin of an ice lobe retreating up the Mackenzie Valley during a period of active retreat. The more parallel, linear-pattern flowsets (Fs 101, 102, 156) were formed further up-ice, away from the margin, and indicate a switch to more northwesterly oriented ice flow in the up-ice portions of the ice stream, compared to the more northerly oriented flow of the earlier flow phase during the LGM (e.g. Fs 90, 101, 102; Figure 6F and G, mid-left). As ice retreated across the Anderson Plain, the northwestern section of the Bear Lake Ice Stream activated (Fs 115; Figure 6F and G, mid-left), and the morphology of the ice flow parallel lineations within this ice stream indicates that it merged with the Mackenzie Trough Ice Stream to the south and the Anderson Ice Stream to the north.

As ice retreated up the Mackenzie Valley, the flow direction was heavily controlled by the local topography with many small ice lobes exhibiting varying flow directions due to the deflection around higher terrain (Fs 175, 179, 180). At the range front of the Canadian Cordillera, the ice flow was directed westwards into the foothills of the Mackenzie Mountains (Fs 3, 4, 5, 19, 20; Figure 6G, bottom-left) and the Richardson Mountains (Fs 161, 162, 167, 171, 172; Figure 6G, top-left).

5.2.5 Timeslice 14.5 ka

High temperatures during the early Bølling-Allerød interval may have triggered the collapse of the ice saddle between the CIS and LIS and rapid ice margin retreat (Gregoire et al., 2016; Stoker et al., 2022). The ice drainage network underwent widespread reorganisation in response to this collapse, with a shift to westerly-oriented ice flow (Figure 6H). During the earlier stages of this timestep, ice flow was still fed by the ice saddle region and directed along the Mackenzie Valley to the north (Fs 23, 34, 39, 309; Figure 6H, bottom-left). In the later stages of this timestep, the ice saddle thinned rapidly and the Keewatin Ice Dome became a more dominant ice source, leading to more westerly-oriented ice flow (e.g. Fs 51, 52, 53, 54; Figure 6H, bottom-left). These changes are also observed in the ice stream network draining through the Amundsen Gulf. The activation of the northwesterly-oriented Paulatuk Ice Stream (Fs-138; Figure 6H, top-left) indicates the increasing importance of the Keewatin Ice Dome as a source area, compared to the Amundsen Gulf Ice Stream at the 15 ka timestep, which maintained clear ice source contribution from the ice saddle as indicated by the northerly-oriented ice flow (Fs 222, 239; Figure 6G, top-right). In the 14.5 ka timestep, we do not depict fast ice flow within the Amundsen Gulf, as the geomorphological evidence for this is likely offshore. This is despite the fact that the Amundsen Gulf Ice Stream may have persisted through this period and was sustained by ice flow from Victoria Island and possibly the Paulatuk Ice Stream (Stokes et al., 2006, 2009; Batchelor et al., 2014; Lakeman et al., 2018).



560 The ice stream network across the Northern Interior Plains displayed a similar shift to north-westwards oriented ice flow as
the Bear Lake Ice Stream and the Fort Simpson Ice Stream became active. We draw an extensive Bear Lake Ice Stream during
this time, but the question remains as to whether the ice stream was active and forming lineations over its entire length at any
single time, or the fast ice flow was concentrated near the ice sheet margin and formed the pattern of lineations time-
transgressively at the margin as it retreated, or a combination of both. Despite the absence of cross-cutting relationships, we
565 suggest that margin retreat was active, with lineations forming time-transgressively near to the ice sheet margin due to two
main reasons. Firstly, the ice stream flowsets at this time are broadly aligned with ice margin retreat landforms (e.g. moraines,
eskers). Secondly, the lineations in the southern portion of the Bear Lake Ice Stream (Fs-65; Figure 6H, mid-image) display a
transition from straight and highly parallel MSGs at higher elevations to a series of sinuous, sometimes paired ridges with
cross-cutting relationships at lower elevations near the Keith Arm of Great Bear Lake (Figure 7). We interpret the lineations
570 at higher elevations as forming beneath grounded ice while the lower elevation lineations formed later by groove-ploughing
from ice keels beneath the partially floating Bear Lake Ice Stream while the ice margin was lightly grounded, following ice
margin retreat and the development of Glacial Lake McConnell (Figure 8; Clark et al., 2003; Piasecka et al., 2018; Dowdeswell
and Ottesen, 2022).

Cross-cutting relationships show that the final ice flow across the Mackenzie Valley was directed to the west as the Bear Lake
575 Ice Stream retreated. Fast ice flow to the northwest in the Mackenzie Valley around 65°N (Fs 83, 312; Figure 6F and G, mid-
left) is overprinted by the large westerly-flowing Bear Lake Ice Stream (Fs-115; Figure 6H, mid-left) and deglacial flowsets
(Fs 94, 95, 96, 97, 157, 162; Figure 6H, mid-left), which display divergent flow patterns indicating the retreat of an ice lobe to
the east. This shift from northwest ice flow to a final westward flow phase is representative of the change in flow direction
observed across the entire region. This eastwards retreat pattern is supported by deglacial flowsets (Fs 106, 107, 108, 109, 110,
580 148; Figure 6H, mid-left), which are aligned with lateral meltwater channels and moraines around the Norman Range.

5.2.6 Timeslice 14.0 ka

Following a period of rapid ice sheet thinning during the saddle collapse, the LIS and CIS had separated along the eastern front
of the Canadian Cordillera by 14.0 ka (Gregoire et al., 2016; Stoker et al., 2022; Dalton et al., 2023). The loss of the ice saddle
585 meant that the Keewatin Ice Dome was the sole ice source for the northwestern sector of the LIS during the subsequent retreat.
Thus, regional ice flow patterns were dominated by broad-scale ice flow towards the west (Figure 6I). Any variation from this
westerly-oriented ice flow was typically caused by the localised deflection of ice flow around higher topography or down the
Mackenzie Valley, including a 180° flow reversal at around 64°N (Fs-26; Figure 6I, centre-left). During this time, the ice sheet
margin continued to rapidly retreat across the Northern Interior Plains (Reyes et al., 2022; Stoker et al., 2022; Dalton et al.,
590 2023) causing rapid adjustments in the ice drainage network. As a result, we depict multiple flow phases within this single
timestep.



At 14 ka, the ice stream network again underwent rapid reorganisations driven by switch-on and shut-down phases for different ice streams. During the early stages of this timestep, the Fort Simpson Ice Stream was active, with a broad convergence zone (Fs-10; Figure 6I, bottom-left) draining ice from the Keewatin Ice Dome. As the westerly ice flow of the Fort Simpson Ice Stream approached the Franklin Mountains and Mackenzie Mountains Foothills, it was deflected to the north by the topographic relief and formed a series of time-transgressive cross-cutting flowsets during deglaciation (Fs 22, 38, 39, 40, 49, 61, 62; Figure 6I, mid-left). The onset zone of the Fort Simpson Ice Stream (Fs-10) is overprinted by the Great Slave Ice Stream (Fs-284; Figure 6I, bottom-left), suggesting that the Great Slave Ice Stream became active following the shut-down of the Fort Simpson Ice Stream in the later stages of this timestep. This likely occurred at the same time ice was flowing over the uplands of Samba K'e (formerly known as Trout Lake; Fs 292, 295, 296; Figure 6I, bottom-left). This sequence of ice stream activity differs from that of Margold et al (2018), who suggested that the Great Slave Ice Stream operated before the Fort Simpson Ice Stream. This was largely due to the constraints of the ice margin chronology of Dyke et al. (2003; updated by Dalton et al., 2023).

At this time, the ice stream activity in the Amundsen Gulf region was reduced as the Paulatuk Ice Stream switched off, and we find no geomorphic evidence of fast ice flow related to the Amundsen Gulf Ice Stream on mainland Canada. Instead, the Amundsen Gulf Ice Stream must have been sustained by ice flow from Victoria Island or had switched-off. Southerly ice flow, around the Horton Plain (Fs-218), indicates the dominance of ice flow from Victoria Island to the north at this time. During retreat, this ice flow became more westerly-oriented and controlled by the topography (Fs-219 and Fs-20 in the 13.5 ka timestep). The Haldane Ice Stream (Fs-129) operated early during this timestep, flowing through the Colville Hills. Following the switch-off of the Haldane Ice Stream, a second flow phase occurred. Overprinting deglacial landforms indicate that ice flow was directed locally to the north around the Colville Hills (Fs-145; Figure 6I, top-left) during the final phase of ice retreat, with geomorphological evidence providing some indication that a readvance may have occurred before final retreat at this location.

615 **5.2.7 Timeslice 13.5 ka**

The northwestern LIS continued to retreat rapidly towards the Canadian Shield across the Northern Interior Plains following ice sheet separation (Reyes et al., 2022; Stoker et al., 2022). As the LIS retreated out of the topographically complex areas in the foothills of the Mackenzie Mountains, ice flow patterns were less complex and dominated by a more consistent westerly flow (Figure 6j). During early stages of this timestep, the only active ice stream was the Great Slave Ice Stream (Fs-284; Figure 6J, bottom-left) because ice flow in the Great Slave Basin was directed towards the west (flow phase 1). As the ice margin retreated, the Great Slave Ice Stream switched-off and ice flow was directed more towards the southwest (flow phase 2; Fs 275, 276, 277; Figure 6J, bottom-left), including Fs-328 which is overprinted on the Great Slave Ice Stream.

In the Horton Plain and Great Bear Plain region, to the north, the ice flow history is more complex due to the influence of the topographic relief and separation of ice sourced from Victoria Island and mainland Canada. North of the Horton Plain, ice



625 flow (Fs-218; Figure 6, top-left) to the southwest indicates the dominance of ice flow from Victoria Island during the final stages of deglaciation. This ice flow gradually became more topographically confined and oriented towards the west (Fs-20; top-left), along the Amundsen Gulf. These flowsets overlap with the margin reconstruction of Dalton et al. (2023) and suggest a more lobate retreat in the Amundsen Gulf at this time aligned with a series of lateral meltwater channels. To the east of the Horton Plain, in the Coronation Hills, the topographic complexity led to complex cross-cutting flow patterns, as indicated by
630 deglacial landforms. These landforms include an esker with flat-topped sections, which displays a morphology similar to examples from Finland where deposition was in an interlobate position (Mäkinen, 2003). Hence, we suggest that this esker formed at the suture zone of two ice masses which were separating over the Coronation Hills. Detailed field investigations would be required to confirm this interpretation. This led to a switch from broadly westerly-oriented ice flow during the early stages of deglaciation, which was unaffected by topography, to a more topographically-confined flow during the later stages
635 of glaciation. Our ice flow sequence in this region matches that of Kleman and Glasser (2007).

5.2.8 Timeslice 13.0 ka

As the LIS retreated onto the Canadian Shield, cosmogenic nuclide dating indicates that the ice margin began to stabilise and the retreat rates slowed (Reyes et al., 2022; Stoker et al., 2022). Across the Canadian Shield, the ice flow was dominated by
640 large-scale radial sheet flow patterns (e.g. Fs 249 and 252; Figure 6K, mid-right) rather than the more complex patterns of rapidly evolving ice streams across the Northern Interior Plains. These flow patterns are broadly independent of the small, local variations in topography. In the northeastern Horton Plain, ice flow is directed parallel to the Amundsen Gulf (Fs 224, 225, 231, 323; Figure 6K, top of image), but the deglacial flowsets suggest a slower ice flow regime. As such, there is no evidence of fast ice flow in the study region at this time. This does not preclude the persistence of the Amundsen Gulf Ice
645 Stream, which might be recorded by evidence of fast ice in the offshore record; slower onshore ice flow directed down the Amundsen Gulf (Fs 224, 225, 231, 323; top of image) may also have contributed to the remnant Amundsen Gulf Ice Stream. Indeed, Margold et al. (2018) inferred that the Amundsen Gulf Ice Stream remained active, based on the assumption that a marine outlet would be conducive to fast ice flow until 11.5 cal. ka BP but with a reduced extent.

650 5.2.9 Timeslice 12.5 ka

The ice flow pattern remained largely unchanged at this time. Across the Canadian Shield, ice flow was dominated by the radial sheet flow from the Keewatin Ice Dome (Figure 6L). The main change in ice flow direction occurred in the Horton Plain region, where deglacial flowsets associated with moraines indicate that the final ice retreat across the area was towards Victoria Island in the northeast (Fs-228, top of image). This either constitutes a minor readvance or simply the last stillstand phase
655 during deglaciation of the region, as previously described in Stokes et al (2006).

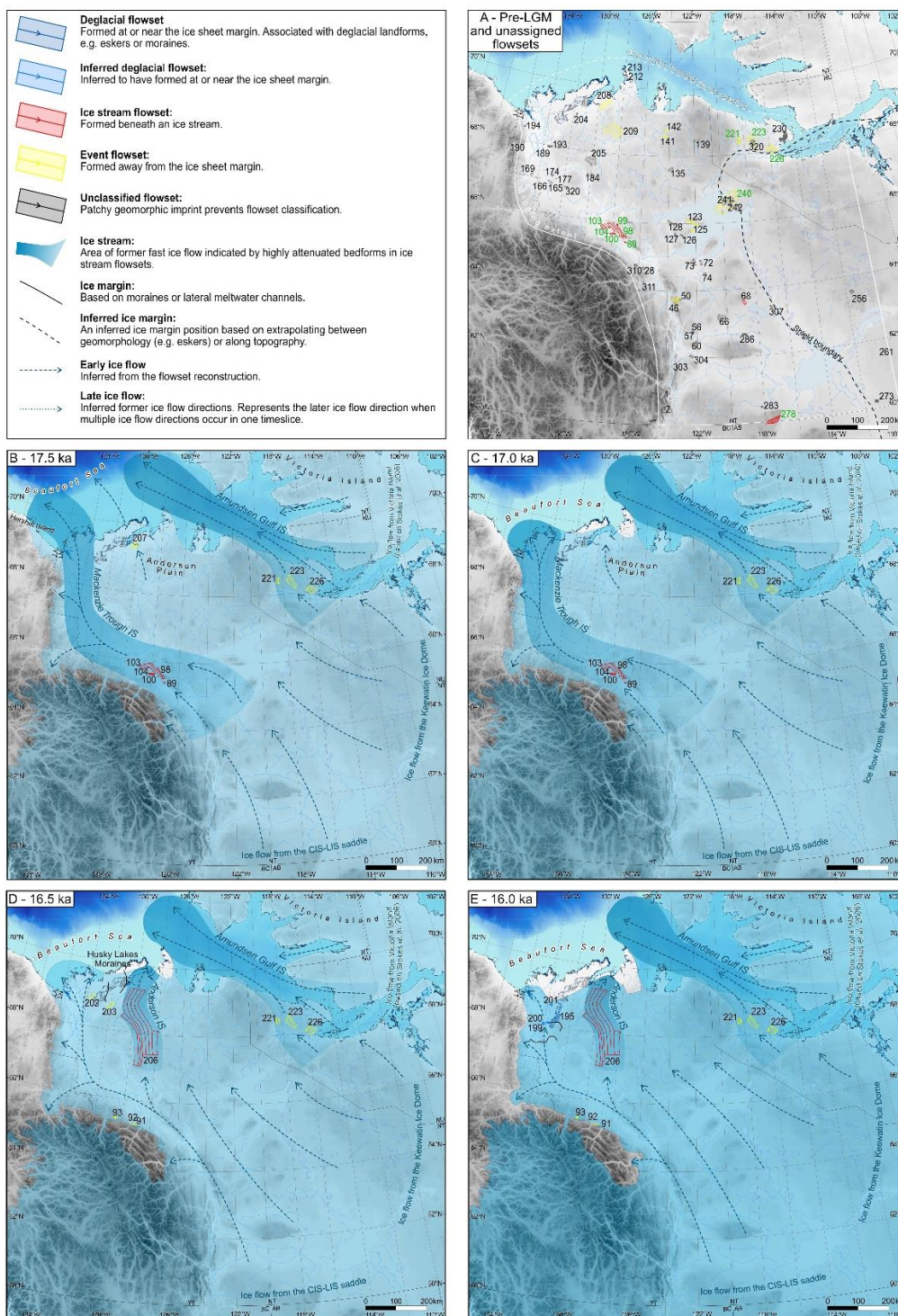


5.2.10 From timeslice 12.0 to 10.5 ka

During the final stages of the slow deglaciation of the study area, ice flow continued to be dominated by broad, radial sheet-flow patterns with small variations of locally deflected ice flow largely controlled by topography (Figure 6M-P). This includes
660 Fs-251 (Figure 6O, centre), which is a smaller radial flowset overprinted on the large Fs-249 (Figure 6K, centre). In the final stage of deglaciation, Fs-250 was overprinted on Fs-251 by a small ice lobe flowing off the Canadian Shield (Figure 6P, top of image). Similarly, Fs-254 is overprinted on Fs-253 and formed following ice margin retreat (Figure 6P, bottom).

5.2.11 Unassigned flowsets

The absence of any cross-cutting patterns or relationships to other geomorphological landforms means that we could not assign
665 the operation of certain flowsets to a specific timestep. There were over forty flowsets which remained unassigned to any timestep and these are predominantly 'unclassified' flowsets and small in spatial extent (Figure 6A). In particular, Fs-230 is somewhat perplexing. It is located in the eastern Horton Plain and displays an ice flow direction towards the northeast, which is at almost 180° to the surrounding flowsets (Fs 229, 231, 232, 233). We cannot reconcile the timing of this flowset with the surrounding features or known ice source areas and suggest it may predate the LGM (Kleman et al., 2010).
670 Remnant ice caps and plateau icefields were left behind following the recession of the southwestern LIS (Norris et al., 2023). While we do not observe any evidence for the presence of localised ice masses following the retreat of the northwestern LIS, we acknowledge the possibility of their presence. Future observations may recognise the presence of local ice masses on the upland of the former bed of the northwestern LIS and might provide an explanation for some of our unassigned flowsets.

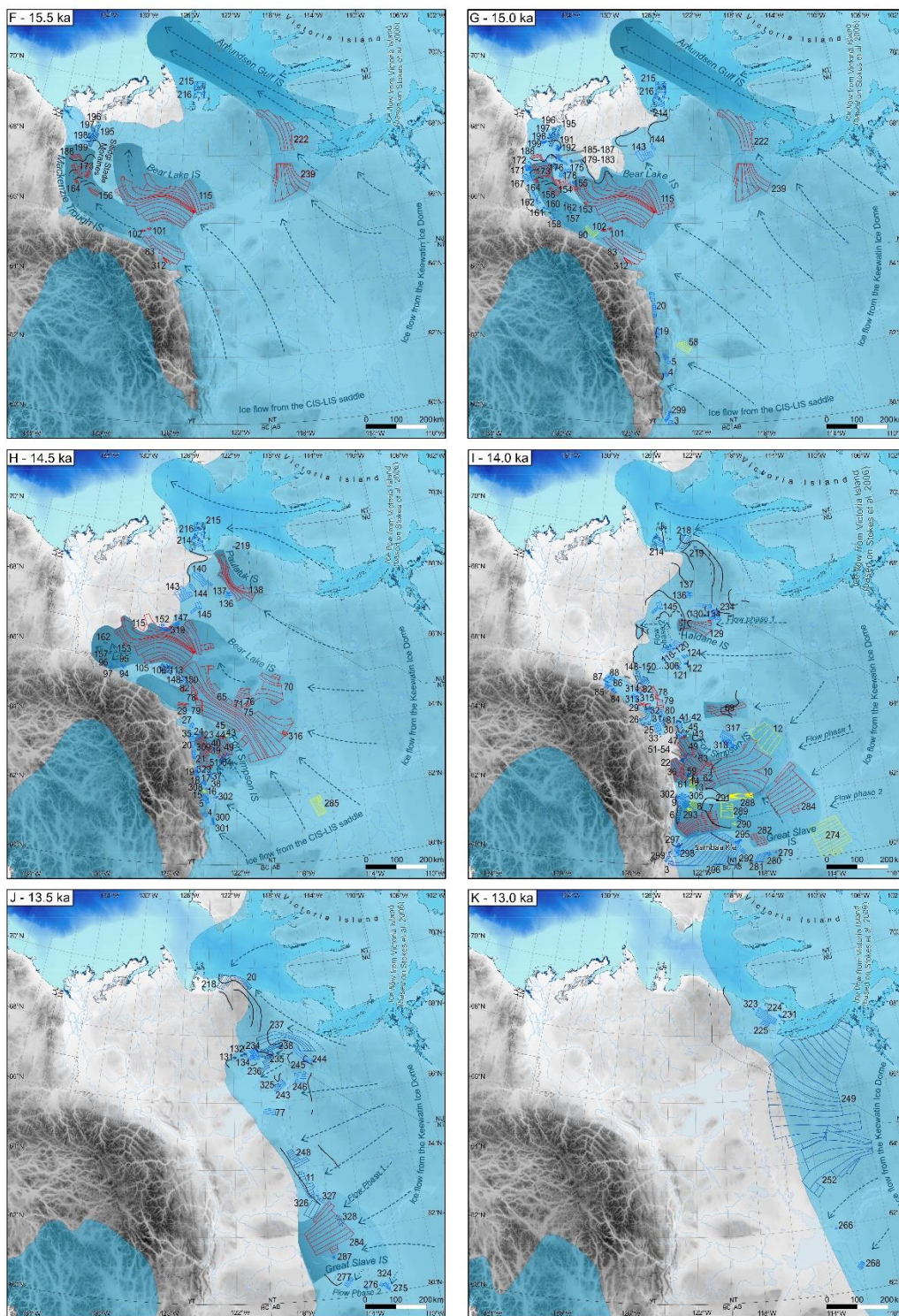


675

Figure 6: The evolution of ice flow using the 500-year timeslices of NADI-1 (Dalton et al., 2023). In panel A, green numbering indicates pre-LGM flowsets and black numbering indicates unclassified flowsets. Due to the size of the



figure, we only number key flowsets. An A4 version of each individual panel is provided in the Supplementary Folder where every flowset is numbered.



680

Figure 6 cont:

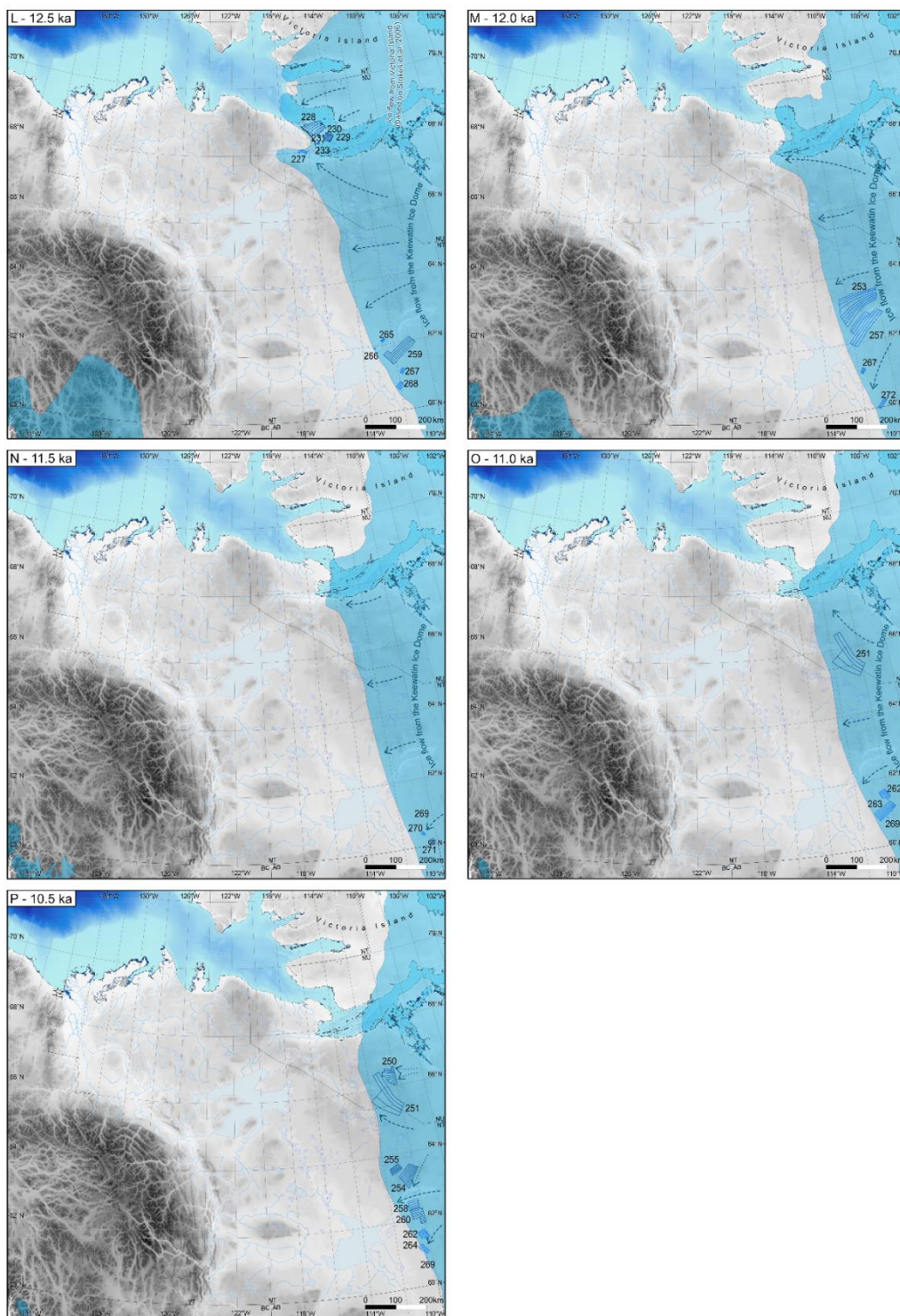
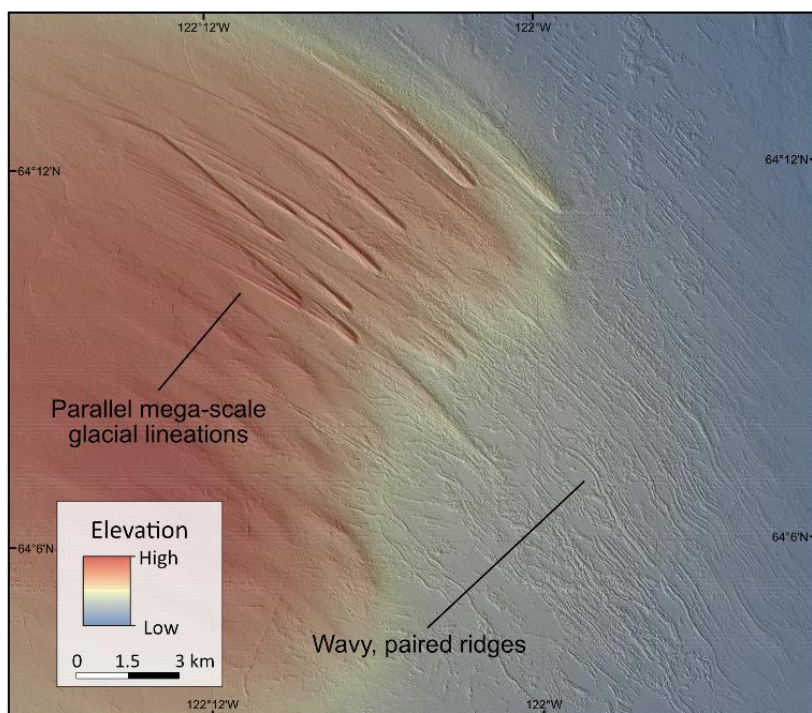


Figure 6 cont:



685

Figure 7: The contrasting lineation morphology around Great Bear Lake. Note how the wavy, sub-parallel lineations at lower elevations differ from the more parallel features at higher elevations which they are overprinted on, probably due to ice flowing in a lightly grounded lacustrine environment.

6 Discussion

690 In our reconstruction, the northwestern LIS undergoes a rapid reconfiguration of its ice drainage network during deglaciation characterized by a change from northerly and northwesterly oriented ice flow at the LGM to westerly-oriented flow during deglaciation. In this section, we discuss the implications of our reconstruction for the changing dominance of ice source regions and how this relates to saddle collapse, the style of ice stream activity, the nature of ice margin retreat processes, the controls on fast ice flow and the implications for ice sheet mass balance.

695

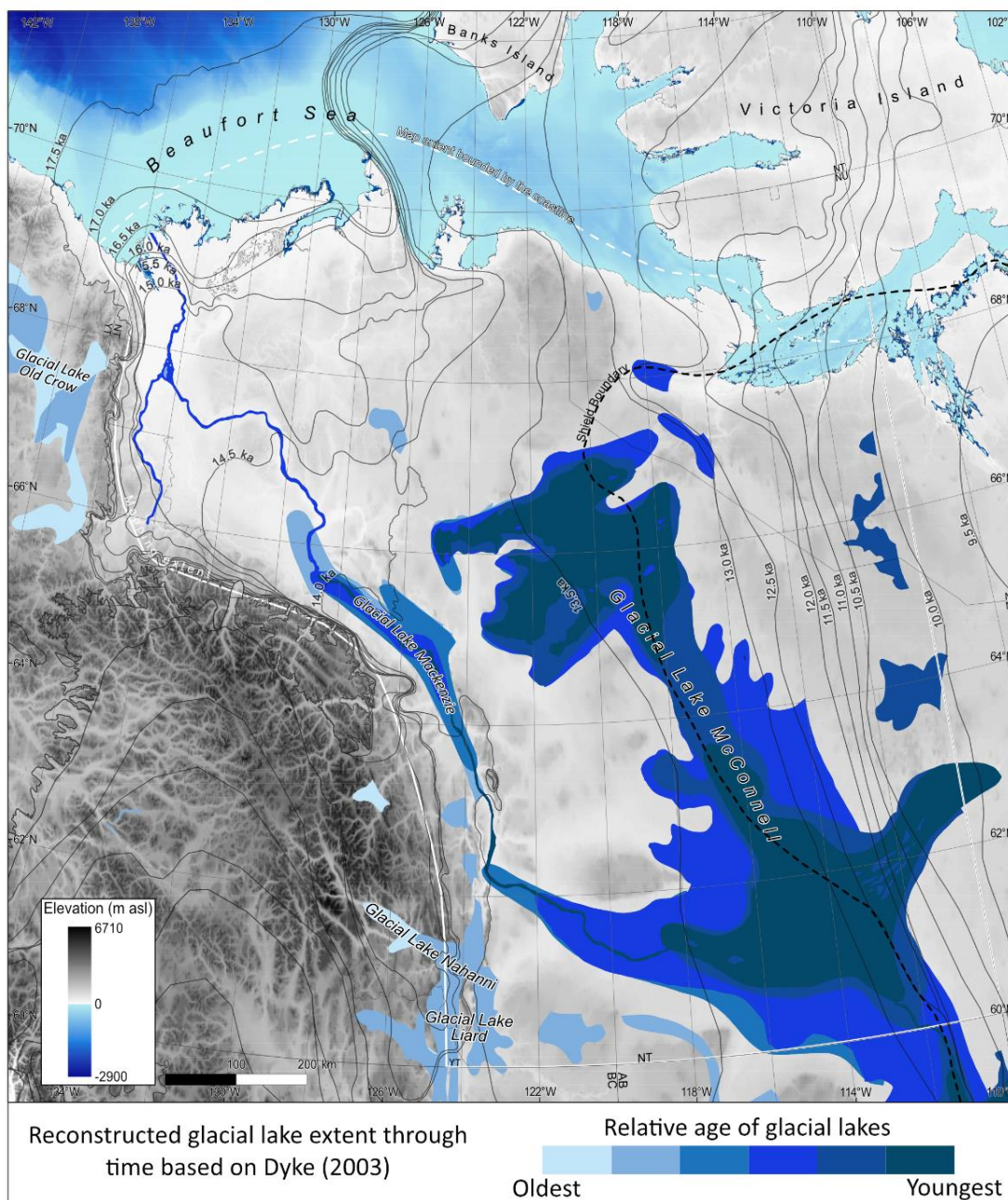


Figure 8: The relative age and extent of proglacial lakes across the study area during the last deglaciation, based on the reconstruction of Dyke et al. (2003). Black lines indicate the deglacial isochrones of Dalton et al. (2023). Note the mismatch between the isochrones and lake reconstruction as the glacial lake reconstruction has not been updated to match the new ice margin chronology.

700



6.1 How did the separation of the ice sheets affect the ice drainage network?

The landform record displays a signal of relatively more rapid rates of thinning in the ice saddle region as the Keewatin Ice Dome became the dominant ice source region. Combined with the available chronological constraints, this provides support for the demise of the ice saddle and separation of the ice sheets occurring before the end of the Bølling–Allerød interval. The dominance of northerly-oriented ice flow at the LGM and the start of deglaciation (Figure 6B–G) demonstrates a strong influence of the Cordilleran-Laurentide ice saddle on the ice drainage network. During the start of the Bølling–Allerød interval, the shift to more northwesterly-oriented ice flow occurs as surface mass balance / elevation feedback causes the rapid thinning of the ice saddle and weakens it relative to the Keewatin Dome (Figure 6H). The ice stream network responds to this change as the Amundsen Gulf Ice Stream (Figure 6G; Fs 222 and 239), with its strong northwards signal, terminates and is replaced by the Paulatuk Ice Stream (Figure 6H; Fs-138) with a more northwesterly ice flow orientation. By the end of the Bølling–Allerød interval, ice flow was broadly westerly-oriented as the ice sheets had separated and the ice saddle had fully collapsed (Figure 6I).

An alternative scenario, where the rapid retreat of the Amundsen Gulf Ice Stream causes ice drawdown from the Keewatin Ice Dome and leads to the collapse of the ice saddle, has been proposed by Pico et al. (2019). This connection between Amundsen Gulf Ice Stream retreat and the ice saddle collapse is based on numerical ice sheet models forced by different palaeotopographies. Based on radiocarbon ages, the collapse of the Amundsen Gulf Ice Stream took place after 13.0 ka and hence is used to suggest that the saddle collapse likely occurred after 13.0 ka (Lakeman et al., 2018; Pico et al., 2019). In fact, it is difficult to envisage a scenario where the Amundsen Gulf Ice Stream is not an important driver of rapid ice drawdown and margin retreat due to the large ice fluxes it likely delivered through the marine terminating margin.

Based on the empirical constraints, we favour the rapid thinning of the ice saddle region as the driver of rapid ice margin retreat across the Northern Interior Plains. The landform record indicates that the final ice flow event in the Mackenzie Valley at ~65°N exhibits a clear southwards deflection around topography, within a broad westerly ice flow pattern from the Keewatin Ice Dome (Fs-25; Figure 6I and 9). Southerly ice flow up the Mackenzie Valley is overprinted on northerly ice flow from the ice saddle region, and therefore is only possible following, the total collapse or significant weakening of the ice saddle, which would otherwise dominate the westward signal of the Keewatin Ice Dome. Both radiocarbon and cosmogenic nuclide exposure age constraints show that the Mackenzie Valley at ~65°N was deglaciated and occupied by Glacial Lake Mackenzie by the end of the Bølling–Allerød interval (Stoker et al., 2022; Dalton et al., 2023). This final ice flow event (Figure 9; Fs 24–26 and 31–32) constrains the separation of the ice sheets to before the Younger Dryas and is incompatible with the scenario proposed by Pico et al. (2019).

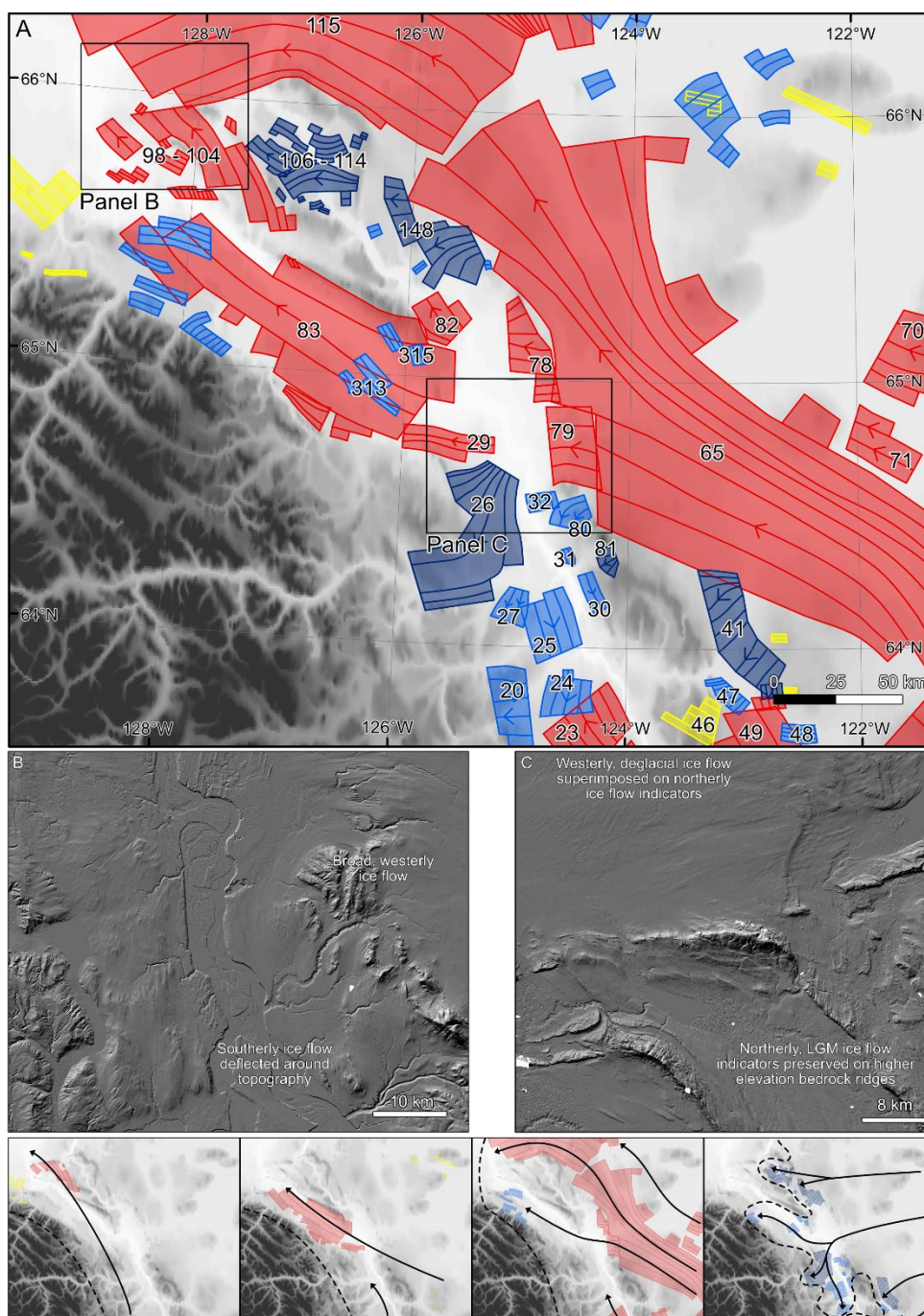


Figure 9: (A) The ice flow patterns in the central Mackenzie Valley. Only key flowsets are numbered and unclassified flowsets are not depicted. (B) Ice flow reversal in the central Mackenzie Valley as broad, westerly ice flow is deflected



735 **around topography in the Mackenzie Valley and (C) fragmented northerly flowsets located on higher elevation bedrock**
ridges that formed during the LGM and are overprinted by the westerly deglacial ice flow in the valley bottom that is
superimposed on the northerly ice flow indicators, note the E-W trending esker which indicates final ice retreat to the
east. The lower panels show a schematic interpretation of the ice flow (black arrows) pattern changes during
deglaciation and approximate ice margins positions (dashed lines). Note, ice margins are purely schematic.

740

6.2 Was deglaciation characterised by dynamic ice margin retreat or more widespread regional stagnation?

The processes of dynamic margin retreat and regional stagnation (i.e. cessation of ice flow and surface downwasting) have both been proposed to explain the style of deglaciation for different regions of the western LIS (Sharpe et al., 2021; Evans et al., 2021; Norris et al., 2023). The model of dynamic ice margin retreat has dominated, especially in broad-scale ice margin
745 reconstructions (Dyke et al., 2003; Dalton et al., 2020), while stagnation has been proposed at a more local scale (Sharpe et al., 2021). Historically, proponents of a dynamic style of ice margin retreat have argued for time-transgressive glacial landforms construction (Wilson, 1939; Dyke and Dredge, 1989) whereas opponents have argued for synchronous landform creation from the margin to distances far up-ice, with the ice sheet subsequently stagnating in place (Shilts et al., 1979; Shilts, 1985; Aylsworth and Shilts, 1989; Brennand, 1994, 2000). This debate has typically considered the processes of active retreat
750 and stagnation as entirely unrelated. Instead, it is perhaps more appropriate to consider the processes of ice margin retreat as a spectrum from active margin retreat (i.e. annual ice margin oscillations indicated by closely spaced, recessional push moraines, such as those developed at temperate Icelandic glaciers; Evans et al., 1999; Chandler et al., 2020) to regional stagnation, with the processes of pulsed recession and punctuated stagnation occurring somewhere in the middle (e.g. Dyke and Evans, 2003; Evans, 2009; Evans et al., 2020; Norris et al., 2023).

755 The retreat pattern of the southwestern LIS margin has recently been divided into three regional zones based on the ice marginal processes that dominated during deglaciation (Norris et al., 2023). Initial deglaciation was characterised by rapid, active ice margin retreat based on the widespread occurrence of recessional push moraines (Norris et al., 2023). An intermediate zone of ice lobe surging and punctuated stagnation, caused by the rapid loss of the ice saddle, is proposed based on the presence of surge landsystem signatures and inter-ice stream zones of hummocky terrain. The final inner zone is characterised by inset
760 push moraines and extensive esker networks, interpreted to indicate a return to active ice retreat. The loss of the ice saddle and the concomitant rapid ice sheet reconfiguration is therein interpreted to have temporarily resulted in surge overprinting and ice stagnation over relatively extensive areas, with active ice retreat resuming once the ice sheet geometry readjusted (cf. Evans et al. 1999, 2008; Norris et al., 2023).

No such broad-scale characterisation of the ice marginal retreat processes and thermal regime exists for the northwestern LIS,
765 but several studies have reconstructed these processes over a smaller geographical area. In the Smoking Hills region, the retreat of the LIS was dominated by pulsed ice-marginal recession and associated punctuated stagnation, evidenced by ice-cored hummocky moraine belts fronted by sharp-crested push moraines. This is an assemblage representative of controlled moraine construction in polythermal ice sheet margins that have undergone local readvances (cf. Dyke & Evans 2003; Evans, 2009;



770 Evans et al., 2021). In contrast, Sharpe et al. (2021) suggest that ice sheet retreat across western Keewatin, to the east of Great Slave Lake, was dominated by regional stagnation. The glacial lineation patterns here are interpreted as forming prior to, not during, deglaciation and a proposed absence of ice marginal landforms is cited as evidence of stagnation. While eskers and meltwater corridors are widespread, they are interpreted as ‘long-conduit’ deposits that form extensively up-ice, especially as there is an absence of associated fans or flat-topped deposits forming esker beads and hence indicative of ice marginal positions (Sharpe et al., 2021).

775 Below, we separate the former bed of the northwestern LIS into three zones. For each zone we outline the thermal regime and processes of ice margin retreat based on the glacial geomorphology depicted in the map of Dulfer et al. (2023).

6.2.1 Retreat style during the early stages of deglaciation (Mackenzie Delta and Anderson Plains region; ~17.5 – 14.5 ka)

780 The deglaciation of the northwestern LIS was dominated by pulsed ice margin retreat, with localised regions of stagnation often limited to upland areas and controlled moraine belts. As outlined above, in the north, controlled moraine arcs lying inboard of sharp-crested push moraines indicate localised readvances of polythermal ice lobes (Evans et al., 2021; Figure 10A); associated with these lobes are overprinted lineation patterns indicative of the warm-based streaming ice located upflow of the frozen snouts (sensu Dyke & Evans 2003). The clearest example of this is in the lower Mackenzie Valley and Mackenzie Delta region, where the Husky Lake thrust moraines indicate the readvance of streaming ice across the Mackenzie Delta to dislocate 785 large masses of ground ice (Dyke and Evans, 2003; Figure 6D). The controlled moraines of the Sitidgi Stade and a series of recessional moraines associated with lobate lineation patterns record pulsed retreat of an ice lobe up the Mackenzie Valley (Figure 6F and G). The varying moraine morphology records complex changes in the thermal regime, as phases of enhanced coupling with the submarginal permafrost resulted in higher fluxes of supraglacial debris via englacial bands and the construction of controlled moraine ridges (Dyke and Evans, 2003). In contrast, isolated regions of higher ground with 790 hummocky terrain may represent localised areas of stagnation as ice on the uplands became separated from the relatively dynamic ice within the valleys (Figure 10B). This suggests that the pulsed style of polythermal ice margin retreat detailed by Evans et al. (2021) was commonplace during the early stages of deglaciation of the northwestern LIS.

6.2.2 Retreat style during the intermediate stage of deglaciation (Northern Interior Plains; ~14.5 – 13.0 ka)

795 The deglaciation style of the central Mackenzie Valley region during the Bølling–Allerød was dominated by rapid, dynamic ice margin retreat. Widespread deglacial flowsets with clear cross-cutting patterns indicate rapid flow reorganisations during the dynamic retreat of the margin. The landforms of the well-established Kelly Lake Phase (Hughes, 1987) provide a clear ice margin location at the edge of the Mackenzie Valley (Figure 6I). Approximately 200 km to the east, a further prominent moraine system indicates the ice margin position towards the end of the Bølling–Allerød (Figure 6J). The recessional moraine sequence around the Norman Range (Figure 10C) and the absence of controlled moraines indicate a transition to warm-based



800 margin conditions may have begun to dominate, in contrast to the early stages of deglaciation, where a complex polythermal regime was dominant.

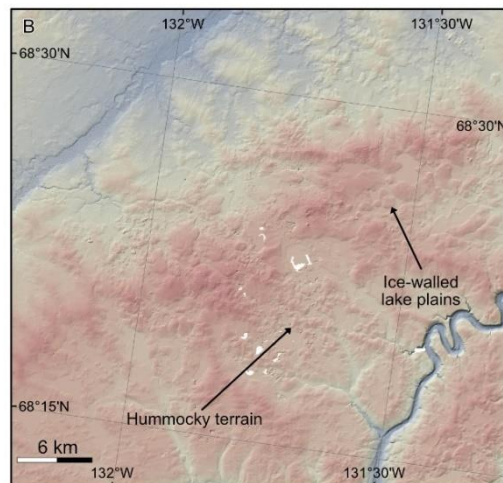
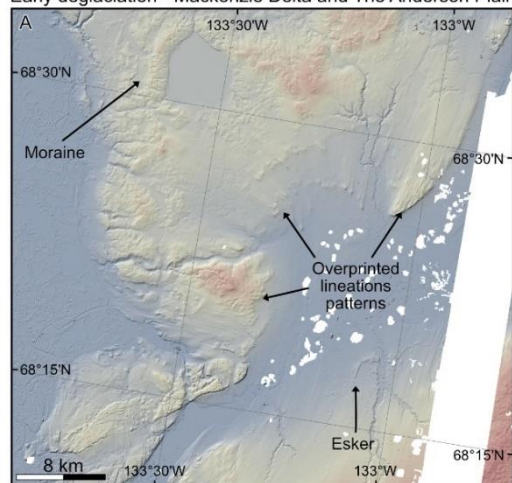
Geomorphological evidence suggests that stagnation was localised during this period, being limited to upland areas bordering former ice streams. Along the terminus of the Bear Lake Ice Stream, extensive networks of crevasse fill ridges associated with Fs-65 (Figure 6H) indicate a rapid shut-down of a possibly surging ice lobe and hummocky terrain with ice-walled lake plains
805 suggest stagnation of ice on the neighbouring uplands (Figure 10D), similar to landsystem signatures reported by Evans et al. (2008, 2016, 2020) for the southwestern LIS. Although, the stagnation is much more localised for the northwestern sector than suggested for the adjacent southwestern sector (Norris et al., 2023). The overprinting of deglacial flowsets wrapping around topographic highs at lower elevations, indicates that ice margin retreat remained relatively active at lower elevations (Figure 6I, Fs-148). In the south of the region, the Liard and Snake Creek moraines record the localised readvance of the LIS margin,
810 driven by the activation and possible surge of the Great Slave Ice Stream (Figure 6I, Fs-7 and 284). At this time, the geomorphological evidence indicates a much greater lobation of the ice sheet margin than depicted by Dalton et al. (2023). While crevasse fill ridges and hummocky terrain on the Sambaa K'e uplands indicate an abrupt shut-down of the Great Slave Ice Stream (Figure 6I), the absence of broad tracts of hummocky terrain in the inter-ice stream regions is interpreted here to suggest that broad regions of ice stagnation were limited. In contrast to the southwestern LIS, where the rapid change in the
815 ice sheet geometry resulted temporarily in relatively extensive ice stagnation (Norris et al., 2023), the northwestern LIS adjusted to the change in ice sheet configuration by dynamic ice margin retreat.

6.2.3 Retreat style during final deglaciation (Canadian Shield; ~13.0 – 10.5 ka)

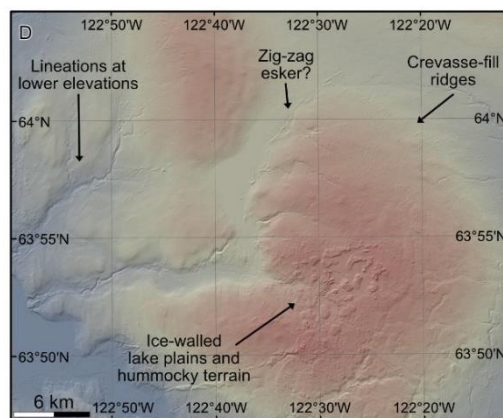
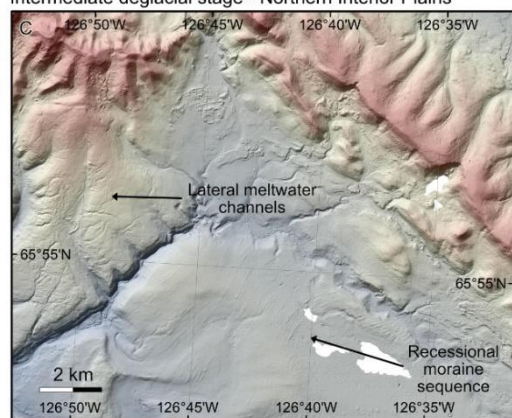
Dynamic ice margin retreat continued as the LIS receded over the Canadian Shield, but the geomorphic expression differed to
820 that of the Northern Interior Plains. On the Canadian Shield to the east of Great Slave Lake, Sharpe et al. (2021) interpreted meltwater corridors and associated eskers and an absence of moraines to indicate that retreat was dominated by regional stagnation of the ice sheet. In contrast, in our study region on the Canadian Shield, flat-topped deposits or fans are commonly observed in association with eskers (Figure 10E and F). Such beaded esker systems are commonly associated with sequential formation of esker segments at or near the ice sheet margin (e.g. Mäkinen, 2003; Stoker et al., 2021). Additionally, overprinting
825 lineation patterns record reorganisations of the ice flow units during deglaciation (Figure 10F). In some locations there is a clearly increasing influence of topography on ice flow, as small ice lobes were developed locally, conflicting with the synchronous formation of lineations proposed further to the east by Sharpe et al. (2021) (Figure 6O, Fs-251; Figure 6P, Fs-250 and 254). Therefore, we suggest that widespread stagnation had not begun for the northwestern LIS margin to the west of 210°W but may have occurred further to the east, as documented by Sharpe et al. (2021). Instead, we propose that pulsed
830 margin retreat likely continued but at lower retreat rates and with slower ice velocities compared to the intermediate stage.



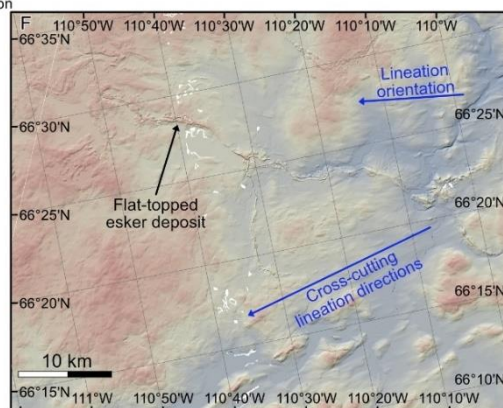
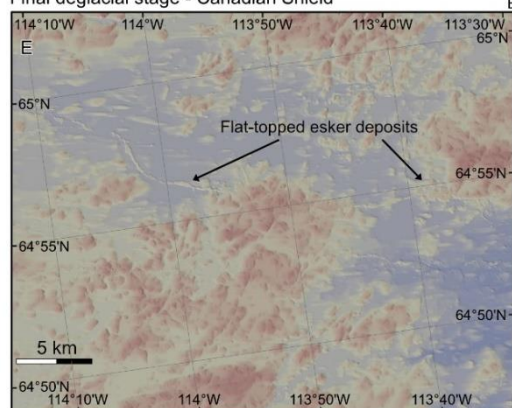
Early deglaciation - Mackenzie Delta and The Anderson Plains



Intermediate deglacial stage - Northern Interior Plains



Final deglacial stage - Canadian Shield



Low High
Elevation

Figure 10: Glacial landforms examples from the former northwestern LIS bed which highlight the contrasting styles of deglaciation across the region. Panel locations are indicated on Figure 1. Note some landforms may only be visible



at higher zoom levels. (A) Overprinting lineation patterns in the Mackenzie Delta region which highlight the changing
835 ice flow directions during dynamic margin retreat to the south. (B) Hummocky terrain on the upland areas of the
Anderson Plain, including ice-walled lake plains, which suggest localised ice stagnation. (C) Recessional moraine
sequence indicating ice margin retreat to the southeast. (D) High-elevation hummocky terrain and crevasse-fill ridges
on the southern edge of the former Bear Lake Ice Stream indicating the rapid shutdown of the ice stream and stagnation
of ice at higher elevations. (E) Flat-topped esker deposits on the Canadian Shield indicating possible former ice margin
840 locations during active ice margin retreat. (F) Cross-cutting lineation pattern on the Canadian Shield indicating the
changing ice flow geometries during retreat.

6.3 How did the ice stream network evolve spatially and temporally during deglaciation?

The extent of fast ice flow back into the ice sheet interior is an important consideration when reconstructing former ice drainage
845 networks and their evolution. The formation of glacial lineations was originally assumed to occur near to the ice sheet margin
(Craig, 1964; Aylsworth and Shilts, 1989), but it is now accepted that lineations can form far behind the ice sheet margin
(Stokes et al., 2009) and, indeed, they have been observed forming 10s of kms up-ice under modern ice streams (King et al.,
2009). Previous reconstructions of the ice streaming activity in the northwestern LIS have highlighted uncertainty over whether
the Mackenzie Trough, Anderson, Bear Lake and Fort Simpson corridors of fast ice flow represent distinct ice streams
850 operating during deglaciation or whether they record a major ice stream system whose drainage route evolved through time
(Brown, 2012; Margold et al., 2015a; 2018; Stokes et al., 2016). These previous reconstructions remain somewhat ambiguous
about the exact configuration of the ice stream network and its extent during deglaciation.

We reconstruct both long and extensive, and shorter, time-transgressive ice streams in the northwestern LIS. The marine-
terminating ice streams operating at the LGM are reconstructed to have penetrated far into the interior of the ice sheet (up to
855 600 km), although the flowsets that serve as the evidence only cover a fraction of the ice stream bed (Fs 89, 98, 100, 103 and
104 in the Mackenzie Trough Ice Stream and Fs 221, 223, 226 in the Amundsen Gulf Ice Stream; Figure 6B). There is also
evidence of the reorganisation of these ice streams during deglaciation (e.g. Fs 101 and 102 in the Mackenzie Trough Ice
Stream and Fs 222 and 239 in the Amundsen Gulf Ice Stream; Figure 6f). These long ice streams remained active during
deglaciation and stepped-back with the margin (Figure 6F, G, H). In this sense, the Mackenzie Trough, Anderson and Bear
860 Lake ice streams represent different generations of the same large ice stream system draining into or towards the western
Beaufort Sea.

The retreat of the ice margin onshore led to the shut-down of these large marine-terminating ice streams and the terrestrial ice
streams that subsequently switched-on were shorter in extent (up to 200 km) and comparably short-lived, existing for only
single timeslices in our reconstruction (e.g. the Haldane Ice Stream, Fs-129; Fort Simpson Ice Stream, Fs-49; Paulatuk Ice
865 Stream, Fs-138). Some terrestrial ice streams, which were lake-terminating (Lemmen et al., 1996; Dyke, 2003; Figure 8) were
larger in size (e.g. Bear Lake Ice Stream, Fs-65 and 115 and the Great Slave Ice Stream, Fs-7 and 284) (Smith, 1992, 1994).
Observations of crevasse-fill ridge networks along the margin of the Bear Lake and Great Slave ice streams may indicate

surge-behaviour and rapid shut-down of these ice streams (cf. Evans et al. 2008, 2016). This differs to the early, long ice streams (Amundsen Gulf and Mackenzie Trough ice streams) which stayed active for as long as 3,000 years during deglaciation and evolved as the ice margin stepped back.

6.4 The influence of ice stream activity on the mass balance of the northwestern LIS

The last glacial termination was characterised by periods of rapid deglaciation interspersed with periods of ice margin stabilization/advance (Figure 11B; Laskar et al., 2004; Rasmussen et al., 2014; Praetorius and Mix., 2014). Global climate oscillations are correlated with and appear to drive these periods of enhanced or reduced rates of ice sheet deglaciation (Lambeck et al., 2014). The precise rates of deglaciation are often non-linearly related to climate, which suggests internal mechanisms may modulate ice sheet retreat rates. As such, there are questions around the relative extent to which past ice margin retreat is controlled by the millennial-scale climatic changes or changes in ice sheet dynamics (Young et al., 2020; Lowell et al., 2021).

The retreat rate of the northwestern LIS shows a clear correlation with these climatic oscillations during retreat across the Northern Interior Plains to the Canadian Shield (Reyes et al., 2022; Stoker et al., 2023). Prior to the Bølling–Allerød interval, ice margin retreat was relatively slow, at less than 100 m/year (Figure 11D). As global temperatures increased during the Bølling–Allerød interval, the ice margin retreat rates increased up to 800 m/year across the Northern Interior Plains and over 350 m/year along Amundsen Gulf (Figure 11, Reyes et al., 2022; Stoker et al., 2022; Dalton et al., 2023). The peak ice margin retreat rates occur towards the middle of the Bølling–Allerød, over 1,000 years after temperatures began to rise (Figure 11). This is because a significant amount of deglaciation occurs through ice sheet thinning (Stoker et al., 2022), while the ice margin retreated relatively slowly. During this time, the ice sheet was characterised by a soft-bed and widespread, ice-marginal glacial lakes (Figure 8). The ice margin stabilised as it retreated onto the Canadian Shield at the start of the Younger Dryas, with retreat rates of less than 100 m/year (Figure 11c and d). The Canadian Shield constitutes a hard subglacial bed and, in our study area, the relative absence of glacial lakes (Figure 8). The ice sheet geometry underwent fundamental reorganisations and changes during this time. We now outline the drivers of changes in ice stream activity across the northwestern LIS and the implications for ice sheet mass balance.

6.4.1 Changes in ice stream activity during retreat across the Northern Interior Plains

Ice stream activity peaked at the start of the Bølling–Allerød Interstadial and then rapidly decreased until no ice streams were active in our study area at the end of the Bølling–Allerød (Figure 11E). Following the local LGM, the ice stream network was stable during generally slow margin retreat (<100 m/year; Figure 11D). Temperature increases prior to, and then more rapidly during, the Bølling–Allerød led to a lowering of the ice sheet surface (Gregoire et al., 2016; Stoker et al., 2022). In the saddle region, this resulted in a rapid expansion of the ablation area and initiated a mass-balance/ice sheet surface elevation feedback, whereby ice sheet thinning lowered larger areas of the ice saddle region to warmer elevations where enhanced melting occurred (Gregoire et al., 2012). This may have caused a steepening of the ice sheet surface profile from the Keewatin Ice Dome and



900 increased driving stresses in ice stream onset areas and the subsequent acceleration of ice streams (Robel and Tziperman, 2016). Through this mechanism, the climatically triggered collapse of the ice saddle can likely explain the peak in ice stream activity observed in the empirical record (Figure 11E and F).

In our reconstruction, the reduction in ice stream activity does not correspond to any climatic or geologic changes (Figure 11). Rather, we suggest ice drawdown created a thinner ice sheet profile and contributed to ice stream slowdown. The low ice
905 surface slope in a thin ice sheet is associated with a reduction in the driving stresses in ice stream onset zones leading to ice stream slowdown (Robel and Tziperman, 2016). Indeed, in other regions of the LIS, ice drawdown during ice streaming has been suggested to cause a thinner ice sheet profile (Stokes and Clark, 2003). As the observed changes ice stream activity (Figure 11) occurred prior to the Younger Dryas cool period and without any observed changes in geological conditions, they are not considered to have influenced the reduction in ice stream activity.

910 Ice stream activity exerts an influence on ice sheet mass balance and may have preconditioned the northwestern LIS for rapid retreat rates across the Northern Interior Plains. Ice stream acceleration is associated with enhanced calving at the ice sheet margin, while ice drawdown from the ice sheet interior to the lower elevation marginal regions causes increased surface melting (Robel and Tziperman, 2016). Broadly speaking, the pervasive fast ice flow and peak in ice stream activity across the Northern Interior Plains between 14.5 and 14.0 ka (Figure 11E) occurs immediately prior to the period of highest ice margin retreat
915 rates. This might indicate that ice drawdown created a thinner ice sheet profile which was vulnerable to rapid retreat (Figure 11D) (Robel and Tziperman, 2016; Gregoire et al., 2016). Previous modelling simulations investigating the influence of saddle collapse on the retreat of the northwestern LIS have not included accurate ice stream processes, despite the fact that they may have contributed to maintaining the high rates of ice margin retreat (Gregoire et al., 2012, 2016). Our observations provide further evidence that ice streaming may be an important factor in maintaining rapid retreat rates during saddle collapse.

920 **6.4.2 The ice flow regime on the Canadian Shield**

Rapid ice drawdown during the peak in ice stream activity during the early Bølling–Allerød meant that the thin ice sheet profile on the Canadian Shield and low driving stresses (Robel and Tziperman, 2016). Ice flow on the Canadian Shield was characterised by a simple radial ice drainage network dominated by a slower flow regime. The transition to a slow flow regime and the reduction in ice stream activity begins at 13.5 ka, before the Younger Dryas and before the ice margin had retreat onto
925 the Canadian Shield (Figure 11). Therefore, we argue that the thin ice sheet profile was the principal reason for the reduction in ice stream activity (Robel and Tziperman, 2016).

The reduction in dynamic mass loss due to this slower ice flow regime might have had a positive impact on the mass balance. Margin stabilisation due to ice dynamics changes and the reduction of the ablation area during cooling in the Younger Dryas may have led to a thickening of the ice sheet (Figure 11C and D). This possible ice sheet thickening is not associated with the
930 re-establishment of ice streaming in our study area. These factors all likely combined to drive ice margin stabilisation and hence the relative importance of climatic versus ice sheet dynamical drivers is difficult to identify.



Our understanding of the magnitude of the regional climatic changes limits our ability to evaluate the influence of climate changes on past ice margin changes. Palaeoenvironmental reconstructions in the Northwest Territories for the period of the Younger Dryas do not show any significant changes in the climate (Ritchie, 1977; Lowdon and Blake, 1981; Rampton, 1988; 935 Spear, 1993). A stable climate during the transition to the Younger Dryas would mean that an alternate driver of the ice margin stabilisation is needed and our reconstructed reduction in ice streaming may have contributed to a positive mass balance and margin stabilisation. Caution is necessary when interpreting past local climatic changes, as the number of studies of Younger Dryas climate in the Northwest Territories are limited and observations from the surrounding regions suggest a cooling period occurred across the Northern Hemisphere (e.g. Praetorius and Mix, 2014). An improved understanding of climate in the 940 Northwest Territories during climate oscillations following the LGM is essential to assess the effects of climate and ice dynamics on the ice sheet retreat rate.

6.4.3 Other factors influencing ice stream activity

Across the study area, mapped ice streams are restricted to locations of soft-bedded conditions and commonly occur where the margin is either lacustrine- or marine-terminating (Figure 8 and 11). Soft-bedded conditions, which dominate across the 945 Northern Interior Plains, are favourable for fast ice flow, as the layer of deformable subglacial sediment enhances subglacial deformation and/or basal sliding (Alley et al., 1986; Winsborrow et al., 2010; Smith et al., 2022). In contrast, the hard-bedded granitic geology of the Canadian Shield provides a greater frictional resistance to ice flow and is resistant to erosion, inhibiting the development of ice streams in the study area (Clark, 1994; Winsborrow et al., 2010). While the climatically-driven changes in the ice sheet geometry are likely the principal control on changing ice stream activity, the subglacial bed conditions across 950 the Northern Interior Plains were favourable for a rapidly developing ice stream system during deglaciation. In contrast, the hard-bed of the Canadian Shield likely contributed to the cessation of ice stream activity.

Increased calving at marine or lacustrine margins encourages increased ice flow velocity and ice draw-down because basal shear stresses are reduced (Stokes and Clark, 2003, 2004; Sutherland et al., 2020; Quiquet et al., 2021; Scherrenberg et al., 2023). Hence, calving margins are an important potential control on the initiation and location of ice stream activity 955 (Winsborrow et al., 2010). The majority of large ice streams (e.g. the Bear Lake and Great Slave Lake ice streams) across the Northern Interior Plains are lacustrine-terminating (Figure 8; Lemmen et al., 1994; Smith, 1994; Dyke et al., 2003; Couch and Eyles, 2008), while the terrestrial ice streams (e.g. the Paulatuk and Haldane ice streams) are typically smaller. This highlights how a calving margin may be important to sustain larger areas of increased ice flow.

At the Canadian Shield boundary, the change to hard-bed conditions and decrease in the proportion of lake-terminating margin 960 likely contributed to the reduction in ice stream activity, but the relative influence of these factors and changes in the ice sheet surface slope are difficult to determine (Figure 11E). While hard-bed conditions are known to exert a stabilising influence on ice flow, large ice streams are observed across the Canadian Shield. The absence of fast ice flow and potential cooling during the Younger Dryas likely led to a thickening of the ice sheet profile but did not lead to the re-establishment of ice stream activity within study area. Ice streaming only occurred after enough time had passed for a significant thickening of the ice



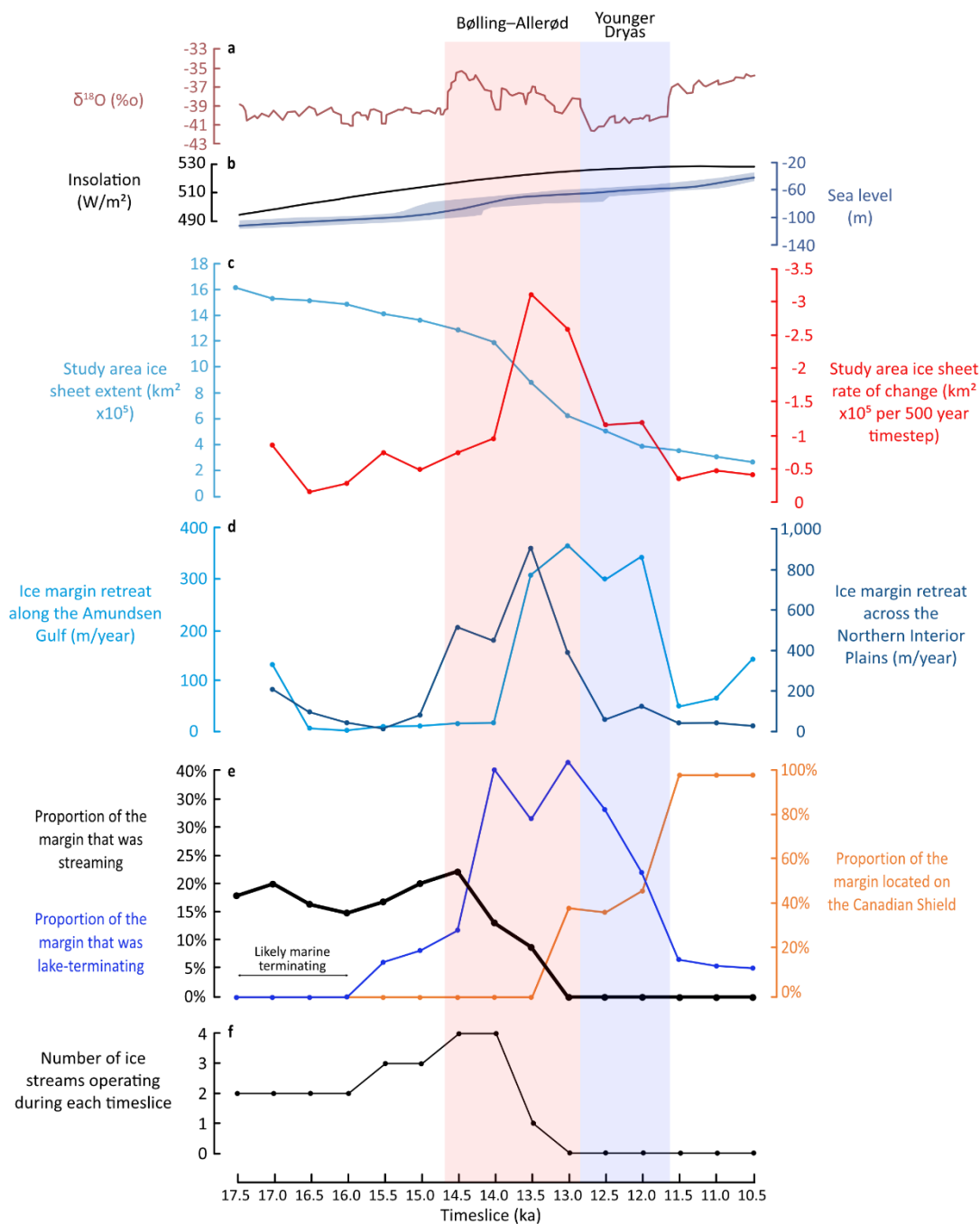
965 sheet profile. The development of the ice-marginal Dubawnt Lake to the east of our study is hypothesised to have triggered the Dubawnt Lake Ice Stream and resulted in rapid ice drawdown due to the steep ice sheet profile in the region, despite hard-bed conditions (Stokes and Clark, 2003, 2004). Similar to the hierarchy of controls on ice streaming set out by Winsborrow et al. (2010), we suggest that glacial lakes are a more important control on ice stream formation than the subglacial geology.

6.4.4 The role of the subglacial drainage system

970 Changes in the meltwater fluxes delivered to the subglacial system and the configuration of the subglacial drainage network have implications for driving fast ice flow (Shabtae and Bentley, 1987; Kamb, 2001; Winsborrow et al., 2010; Margold et al., 2018). High subglacial water pressures can decouple the ice sheet from the bed and facilitate fast ice flow (Clayton et al., 1985, Zwally et al., 2002) but increased channelisation of the drainage network during the deglaciation of the LIS has been associated with a decrease in ice streaming (Storrar et al., 2014). Changes in meltwater production must have influenced the ice streaming
975 of the northwest LIS, but these changes are difficult to accurately reconstruct. For example, during the Younger Dryas, cooler temperatures may have reduced the meltwater production and the delivery to the subglacial system, contributing to the cessation of ice stream activity. However, reconstructing these changes from the empirical record is difficult we are thus unable to accurately establish the importance of the subglacial meltwater drainage.

6.4.5 Summary

980 Atmospheric warming caused increases in the ice sheet surface slope during deglaciation and is interpreted to be the primary control on changes in ice stream activity, with glacial lakes and the subglacial bed conditions playing a secondary role. The increase in driving stresses in ice stream onset zones due to the steepening of the ice sheet surface profile during saddle collapse provides a mechanism to explain the peak in ice stream activity during the Bølling–Allerød. The increased ice draw-down during this peak in ice stream activity ultimately led to lower surface slopes and the reduction in driving stresses which is
985 associated with the reconstructed decline in ice stream activity towards the end of the Bølling–Allerød and before any observed climatic cooling or geological changes. The cessation of ice stream activity due to the thin ice sheet profile continued until the ice sheet had retreated beyond our study area. As climate cooled during the Younger Dryas the reduction of the ablation area likely led to a thickening of the ice sheet, but the shallower ice surface profile following the rapid ice draw-down during the Bølling–Allerød meant that ice stream activity lagged this climatic change (Robel and Tziperman, 2016). During this time,
990 calving into large proglacial lakes and a subglacial soft-bed played a secondary role by facilitating ice streaming and controlling the distribution and size of ice streams.



995 **Figure 11: (A)** $\delta^{18}\text{O}$ record from the Greenland GRIP ice core displayed in red (Rasmussen et al., 2014; Seierstad et al., 2014), **(B)** Relative sea level curve is blue is adapted from Carlson and Clark (2012) and based on a compilation of far-field sites and the mean summer insolation at 65°N is in black (Laskar et al., 2004). **(C)** The total extent of the LIS (blue line) in our study area (displayed in Figure 1) at each 500-year timestep covered in our reconstruction, based upon the



reconstruction of Dalton et al. (2023). When the ice sheets were merged, the extent was calculated east of 127°W. The rate of ice sheet area loss per 500-year timestep is displayed in red. (D) The rate of ice margin retreat along two separate transects (displayed in Figure 1) for each 500-year timestep. (E) The proportion of the ice sheet margin in the study area that was streaming (thick black line) at each 500-year timestep based on our reconstruction (Figure 6). The proportion of the ice sheet margin that was lake-terminating (blue; calculated by measuring the extent of the ice margin from the reconstruction of Dalton et al (2023) that is located in an area of glacial lake extent from Dyke et al. (2003)) and the proportion of the ice sheet margin that is located on the hard-bedded Canadian Shield for each 500-year timestep (orange). (F) The total number of ice streams operating at each timestep of our reconstruction (Figure 6).

7 Conclusions

Using the glacial geomorphological map of Dulfer et al. (2023) we apply the established practice of flowset mapping and the glacial inversion method to reconstruct the ice flow evolution of the northwestern Laurentide Ice Sheet and ice margin retreat processes and patterns at 500-year intervals. We categorise over 300 flowsets based on lineation morphology, orientation, patterns of overprinting and their relationship with other landforms.

The ice margin retreat of the northwestern LIS was dominated by pulsed recession of the margin, with stagnation restricted to localised areas as buried ice melts out from controlled moraine deposits and on isolated uplands. In the early stages of deglaciation of the Northern Interior Plains, widespread controlled moraines record the pulsed recession of a polythermal margin, with sharp ridges and push moraines marking the extent of readvances of this margin. To the south of ~66°N, widely spaced, sharp-crested push moraines record the rapid retreat of a polythermal margin. A localised patch of recessional moraines around the Norman Range records the active retreat of a warm-based portion of the margin. Stagnation is limited to the upland inter-ice stream areas, which became disconnected from the dynamic ice at lower elevations. Although, regional stagnation has previously been suggested (Sharpe et al., 2021) for the deglaciation of the LIS margin across western Keewatin, we do not observe any indicators of widespread stagnation across the Canadian Shield. If widespread stagnation of the margin occurred, we suggest that it must have occurred after the LIS retreated to the east of 110°W.

We identify rapid changes in the ice drainage geometry and network, whereby predominantly northerly LGM ice flow from the Cordilleran-Laurentide ice saddle transitioned to a westwards ice flow from the Keewatin Ice Dome over a period of just 2000 years. The reorganisation of the ice drainage network is consistent with rapid thinning in the ice saddle region, driven by surface mass balance feedbacks, compared to a slower deglaciation of the Keewatin Ice Dome. The increased driving stresses due to the oversteepening of the ice sheet surface profile during the rapid thinning of the ice saddle provides a mechanism to understand the peak in ice stream activity during the Bølling–Allerød interval. The ice draw-down from the Keewatin Ice Dome following this peak in ice stream activity may have lowered the ice sheet surface profile and led to a reduction of ice stream activity towards the end of the Bølling–Allerød interval. During deglaciation, the presence of lacustrine calving margins and soft-bedded subglacial conditions appear to play a modulating role on ice stream activity. As the ice sheet retreated on to



1030 the Canadian Shield, the relative absence of a calving margin and hard-bedded conditions likely combined with climatically-
driven changes in the ice sheet surface profile to cause the complete cessation of ice stream activity in our study region.
Numerical ice sheet modelling studies have not yet fully captured the role of ice streaming processes when simulating the
collapse of the Cordilleran-Laurentide ice saddle. Our mapping results and reconstruction might provide a useful template for
guiding and testing modelling experiments and we suggest future studies could aim to better represent ice streaming processes
1035 to investigate the drivers of rapid ice sheet retreat in the region.

Data availability

The data referred to in this paper have all been provided within the tables and figures in the main text and in the Supplement.
The supplementary materials related to this article are available in the Supplement and
at <https://doi.org/10.6084/m9.figshare.25003559.v1>.

1040 Funding sources

BJS and HED acknowledge support by the project Grant Schemes at Charles University (reg. no. CZ.02.2.69/0.0/0.0/19_073/0016935; START/SCI/055). BJS and HED were fully supported by the START research project during all stages of this work. CDC was supported by the European Research Council, H2020 (PalGlac grant no. 787263). DF
1045 was supported by grants from the Natural Science and Engineering Research Council of Canada and Natural Resources Canada Polar Continental Shelf Program.

Competing interests

At least one of the (co-)authors is a member of the editorial board of The Cryosphere.

Acknowledgements

This study area covers the territories of many First Nations communities across the Northwest Territories and Nunavut and we
1050 acknowledge the First Nations people as the traditional owners of the land. We thank Rod Smith who helped shape the
manuscript through multiple discussions and conversations.



References

- Alley, R.B., Blankenship, D.D., Bentley, C.R. and Rooney, S.T., 1986. Deformation of till beneath ice stream B, West Antarctica. *Nature*, 322(6074), pp.57-59
- Aylsworth, J.M., and Shilts, W.W. 1989. Glacial features around the Keewatin Ice Divide: Districts of Mackenzie and Keewatin. Geological Survey of Canada. Paper 88-24, 21. p.
- Bamber, J.L., Vaughan, D.G. and Joughin, I., 2000. Widespread complex flow in the interior of the Antarctic ice sheet. *Science*, 287(5456), pp.1248-1250
- Batchelor, C.L., Dowdeswell, J.A. and Pietras, J.T., 2013. Seismic stratigraphy, sedimentary architecture and palaeo-glaciology of the Mackenzie Trough: evidence for two Quaternary ice advances and limited fan development on the western Canadian Beaufort Sea margin. *Quaternary Science Reviews*, 65, pp.73-87
- Batchelor, C.L., Dowdeswell, J.A. and Pietras, J.T., 2014. Evidence for multiple Quaternary ice advances and fan development from the Amundsen Gulf cross-shelf trough and slope, Canadian Beaufort Sea margin. *Marine and Petroleum Geology*, 52, pp.125-143
- Batchelor, C.L., Margold, M., Krapp, M., Murton, D.K., Dalton, A.S., Gibbard, P.L., Stokes, C.R., Murton, J.B. and Manica, A. (2019) The configuration of Northern Hemisphere ice sheets through the Quaternary. *Nature Communications* 10, 3713.
- Bateman, M.D. and Murton, J.B., 2006. The chronostratigraphy of Late Pleistocene glacial and periglacial aeolian activity in the Tuktoyaktuk Coastlands, NWT, Canada. *Quaternary Science Reviews*, 25(19-20), pp.2552-2568
- Bednarski, J. M., 2002. *Surficial geology, Fisherman Lake, Northwest Territories – Yukon Territory*. Geological Survey of Canada, Open File 4360, scale 1:50,000. <https://doi.org/10.4095/213653>.
- Bednarski, J. M., 2003a. *Surficial geology, Arrowhead Lake, Northwest Territories*. Geological Survey of Canada, Open File 1775, scale 1:50,000. <https://doi.org/10.4095/214449>.
- Bednarski, J. M., 2003b. *Surficial geology, Arrowhead River, Northwest Territories*. Geological Survey of Canada, Open File 4483, scale 1:50,000. <https://doi.org/10.4095/214618>.
- Bednarski, J. M., 2003c. *Surficial geology, Betalamea Lake, Northwest Territories – Yukon Territory*. Geological Survey of Canada, Open File 4502, scale 1:50,000. <https://doi.org/10.4095/214790>.
- Bednarski, J. M., 2003d. *Surficial geology, Celibeta Lake, Northwest Territories – British Columbia*. Geological Survey of Canada, Open File 1754, scale 1:50,000. <https://doi.org/10.4095/214417>.
- Bednarski, J. M., 2003e. *Surficial geology, Denedothada Creek, Northwest Territories*. Geological Survey of Canada, Open File 4480, scale 1:50,000. <https://doi.org/10.4095/214603>.
- Bednarski, J. M., 2003f. *Surficial geology, Emile Lake, Northwest Territories*. Geological Survey of Canada, Open File 4477, scale 1:50,000. <https://doi.org/10.4095/214560>.
- Bednarski, J. M., 2003g. *Surficial geology, Fort Liard, Northwest Territories – British Columbia*. Geological Survey of Canada, Open File 1760, scale 1:50,000. <https://doi.org/10.4095/214418>.



- Bednarski, J. M., 2003h. *Surficial geology, Lake Bovie, Northwest Territories – British Columbia*. Geological Survey of Canada, Open File 1761, scale 1:50,000. <https://doi.org/10.4095/214419>.
- Bednarski, J. M., 2003i. *Surficial geology, Mount Flett, Northwest Territories*. Geological Survey of Canada, Open File 4481, scale 1:50,000. <https://doi.org/10.4095/214617>.
- 1090 Bednarski, J. M., 2003j. *Surficial geology, Muskeg River, Northwest Territories*. Geological Survey of Canada, Open File 1753, scale 1:50,000. <https://doi.org/10.4095/214408>.
- Bednarski, J. M., 2003k. *Surficial geology, Netla River, Northwest Territories*. Geological Survey of Canada, Open File 4478, scale 1:50,000. <https://doi.org/10.4095/214561>.
- Bednarski, J. M., 2003l. *Surficial geology, Pointe-de-fleche River, Northwest Territories*. Geological Survey of Canada, Open
1095 File 1773, scale 1:50,000. <https://doi.org/10.4095/214763>.
- Bednarski, J. M., 2003m. *Surficial geology, Rabbit Creek, Northwest Territories*. Geological Survey of Canada, Open File 4486, scale 1:50,000. <https://doi.org/10.4095/214644>.
- Bednarski, J. M., 2003n. *Surficial geology, Sawmill Mountain, Northwest Territories*. Geological Survey of Canada, Open File 4476, scale 1:50,000. <https://doi.org/10.4095/214528>.
- 1100 Bednarski, J. M., 2003o. *Surficial geology, Tourbiere River, Northwest Territories*. Geological Survey of Canada, Open File 4487, scale 1:50,000. <https://doi.org/10.4095/214682>.
- Bednarski, J. M., 2008. Landform assemblages produced by the Laurentide Ice Sheet in northeastern British Columbia and adjacent Northwest Territories – constraints on glacial lakes and patterns of ice retreat. *Canadian Journal of Earth Sciences*, *45*, 593–610. <https://doi.org/10.1139/E07-053>
- 1105 Bednarski, J.M. and Smith, I.R., 2007. Laurentide and montane glaciation along the Rocky Mountain Foothills of northeastern British Columbia. *Canadian Journal of Earth Sciences*, *44*(4), pp.445-457
- Beget, J., 1987. Low profile of the Northwest Laurentide Ice Sheet. *Arctic and Alpine Research*, *19*, No. 1, 81-88.
- Benn, D.I., & Evans, D.J.A., 2010. *Glaciers and glaciation* (2nd ed.). Routledge.
- Bennett, M.R., 2003. Ice streams as the arteries of an ice sheet: their mechanics, stability and significance. *Earth-Science
1110 Reviews*, *61*(3-4), pp.309-339
- Boulton, G.S. and Clark, C.D., 1990. The Laurentide ice sheet through the last glacial cycle: the topology of drift lineations as a key to the dynamic behaviour of former ice sheets. *Earth and Environmental Science Transactions of The Royal Society of Edinburgh*, *81*(4), pp.327-347
- Brennand, T.A., 1994. Macroforms, large bedforms and rhythmic sedimentary sequences in subglacial eskers, south-central
1115 Ontario: implications for esker genesis and meltwater regime. *Sedimentary Geology*, *91*(1-4), pp.9-55
- Brennand, T.A., 2000. Deglacial meltwater drainage and glaciodynamics: inferences from Laurentide eskers, Canada. *Geomorphology*, *32*(3-4), pp.263-293
- Brown, V., 2012. *Ice stream dynamics and pro-glacial lake evolution along the north-western margin of the Laurentide Ice Sheet* (Doctoral dissertation, Durham University).



- 1120 Brown, V.H., Stokes, C.R. and Ó Cofaigh, C., 2011. The glacial geomorphology of the north-west sector of the Laurentide Ice Sheet. *Journal of Maps*, 7(1), pp.409-428
- Carlson, A.E. and Clark, P.U., 2012. Ice sheet sources of sea level rise and freshwater discharge during the last deglaciation. *Reviews of Geophysics*, 50(4)
- Chandler, B.M., Chandler, S.J., Evans, D.J.A., Ewertowski, M.W., Lovell, H., Roberts, D.H., Schaefer, M. and Tomczyk, A.M.,
1125 2020. Sub-annual moraine formation at an active temperate Icelandic glacier. *Earth Surface Processes and Landforms*, 45(7), pp.1622-1643
- Chandler, B.M., Lovell, H., Boston, C.M., Lukas, S., Barr, I.D., Benediktsson, Í.Ö., Benn, D.I., Clark, C.D., Darvill, C.M., Evans, D.J.A. and Ewertowski, M.W., 2018. Glacial geomorphological mapping: A review of approaches and frameworks for best practice. *Earth-Science Reviews*, 185, pp.806-846
- 1130 Clark, C.D., 1993. Mega-scale glacial lineations and cross-cutting ice-flow landforms. *Earth surface processes and landforms*, 18(1), pp.1-29
- Clark, C.D., 1997. Reconstructing the evolutionary dynamics of former ice sheets using multi-temporal evidence, remote sensing and GIS. *Quaternary Science Reviews*, 16(9), pp.1067-1092
- Clark, C.D., 1999. Glaciodynamic context of subglacial bedform generation and preservation. *Annals of Glaciology*, 28, pp.23-
1135 32
- Clark, C.D., Ely, J.C., Hindmarsh, R.C., Bradley, S., Ignéczi, A., Fabel, D., Ó Cofaigh, C., Chiverrell, R.C., Scourse, J., Benetti, S. and Bradwell, T., 2022. Growth and retreat of the last British–Irish Ice Sheet, 31 000 to 15 000 years ago: the BRITICE-CHRONO reconstruction. *Boreas*, 51(4), pp.699-758
- Clark, C.D., Hughes, A.L., Greenwood, S.L., Jordan, C. and Sejrup, H.P., 2012. Pattern and timing of retreat of the last British-
1140 Irish Ice Sheet. *Quaternary Science Reviews*, 44, pp.112-146
- Clark, C.D., Knight, J.K. and Gray, J.T., 2000. Geomorphological reconstruction of the Labrador sector of the Laurentide Ice Sheet. *Quaternary Science Reviews*, 19(13), pp.1343-1366
- Clark, C.D., Tulaczyk, S.M., Stokes, C.R. and Canals, M., 2003. A groove-ploughing theory for the production of mega-scale glacial lineations, and implications for ice-stream mechanics. *Journal of Glaciology*, 49(165), pp.240-256
- 1145 Clark, P.U., 1994. Unstable behavior of the Laurentide Ice Sheet over deforming sediment and its implications for climate change. *Quaternary Research*, 41(1), pp.19-25
- Clark, P.U., Dyke, A.S., Shakun, J.D., Carlson, A.E., Clark, J., Wohlfarth, B., Mitrovica, J.X., Hostetler, S.W. and McCabe, A.M., 2009. The Last Glacial Maximum. *Science*, 325(5941), pp.710-714
- Clayton, L., Teller, J.T. and Attig, J.W., 1985. Surging of the southwestern part of the Laurentide Ice Sheet. *Boreas*, 14(3),
1150 pp.235-241
- Couch, A.G. and Eyles, N., 2008. Sedimentary record of glacial lake Mackenzie, Northwest Territories, Canada: Implications for Arctic freshwater forcing. *Palaeogeography, Palaeoclimatology, Palaeoecology*, 268(1-2), pp.26-38
- Craig, B.G. 1964. *Surficial geology of east-central District of Mackenzie*. Geological Survey of Canada. *Bulletin*, 99: 41.p.



- 1155 Dalton, A.S., Dulfer, H.E., Margold, M., Heyman, J., Clague, J.J., Froese, D.G., Gauthier, M.S., Hughes, A.L.C., Jennings, C.E., Norris, S.L., and Stoker, B.J., 2023. Deglaciation of the North American Ice Sheet Complex in calendar years based on a new comprehensive database of chronological data: NADI-1. *Quaternary Science Reviews*.
- Dalton, A.S., Margold, M., Stokes, C.R., Tarasov, L., Dyke, A.S., Adams, R.S., Allard, S., Arends, H.E., Atkinson, N., Attig, J.W. and Barnett, P.J., 2020. An updated radiocarbon-based ice margin chronology for the last deglaciation of the North American Ice Sheet Complex. *Quaternary Science Reviews*, 234, p.106223
- 1160 De Angelis, H. and Kleman, J., 2005. Palaeo-ice streams in the northern Keewatin sector of the Laurentide ice sheet. *Annals of Glaciology*, 42, pp.135-144
- De Angelis, H. and Kleman, J., 2007. Palaeo-ice streams in the Foxe/Baffin sector of the Laurentide Ice Sheet. *Quaternary Science Reviews*, 26(9-10), pp.1313-1331
- Dowdeswell, J.A. and Ottesen, D., 2022. Geomorphic signature of the presence and breakup of large ice-sheet derived multi-keeled tabular icebergs. *Marine Geology*, 451, p.106889
- 1165 Duk-Rodkin, A. and Hughes, O.L., 1991. Age relationships of Laurentide and montane glaciations, Mackenzie Mountains, Northwest territories. *Géographie physique et Quaternaire*, 45(1), pp.79-90
- Duk-Rodkin, A., 1999. *Glacial limits map of Yukon*. Geological Survey of Canada, Open File 3694
- Duk-Rodkin, A., 2022. *Glacial limits, Mackenzie Mountains and foothills, Northwest Territories, Canada*. Geological Survey of Canada, Open File 8891.
- 1170 Duk-Rodkin, A., Barendregt, R.W., Froese, D.G., Weber, F., Enkin, R., Smith, I.R., Zazula, G.D., Waters, P. and Klassen, R., 2004. Timing and extent of Plio-Pleistocene glaciations in north-western Canada and east-central Alaska. In *Developments in Quaternary Sciences* (Vol. 2, pp. 313-345). Elsevier.
- Duk-Rodkin, A., Barendregt, R.W., Tarnocai, C. and Phillips, F.M., 1996. Late Tertiary to late Quaternary record in the Mackenzie Mountains, Northwest Territories, Canada: stratigraphy, paleosols, paleomagnetism, and chlorine-36. *Canadian Journal of Earth Sciences*, 33(6), pp.875-895
- 1175 Dulfer, H.E., Stoker, B.J., Margold, M., and Stokes, C.R., 2023. Glacial geomorphology of the northwest Laurentide Ice Sheet on the northern Interior Plains and western Canadian Shield, Canada. *Journal of Maps*.
- Dyke, A.S., 2004. An outline of the deglaciation of North America with emphasis on central and northern Canada. *Quaternary Glaciations Extent and Chronology, Part II: North America. Developments in Quaternary Science*, 2
- 1180 Dyke, A. S., Moore, A., & Robertson, L., 2003. Deglaciation of North America. *Ottawa: Geological Survey of Canada*.
- Dyke, A.S. and Evans, D.J.A., 2003. Ice-marginal terrestrial landsystems: northern Laurentide and Inuitian ice sheet margins. In: Evans, D.J.A. (ed.), *Glacial landsystems* (pp. 143-165). Routledge
- Dyke, A.S., Andrews, J.T., Clark, P.U., England, J.H., Miller, G.H., Shaw, J. and Veillette, J.J., 2002. The Laurentide and Inuitian ice sheets during the last glacial maximum. *Quaternary Science Reviews*, 21(1-3), pp.9-31
- 1185



- Dyke, A.S., and Dredge, L.A., 1989. Quaternary geology of the northwestern Canadian Shield, Chap. 3: Quaternary geology of the Canadian Shield. In *Quaternary Geology of Canada Greenland*. Edited by R.J. Fulton. Geological Survey of Canada, Geology of Canada Series No. 1, 1989, pp. 189–214. <https://doi.org/10.4095/127963>.
- England, J., Atkinson, N., Bednarski, J., Dyke, A.S., Hodgson, D.A. and Cofaigh, C.Ó., 2006. The Innuitian Ice Sheet: configuration, dynamics and chronology. *Quaternary Science Reviews*, 25(7-8), pp.689-703
- 1190 Evans, D.J.A, 2009. Controlled moraines: origins, characteristics and palaeoglaciological implications. *Quaternary Science Reviews*, 28(3-4), pp.183-208
- Evans, D.J.A, Atkinson, N. and Phillips, E., 2020. Glacial geomorphology of the Neutral Hills Uplands, southeast Alberta, Canada: The process-form imprints of dynamic ice streams and surging ice lobes. *Geomorphology*, 350, p.106910
- 1195 Evans, D.J.A, Clark, C.D. and Rea, B.R., 2008. Landform and sediment imprints of fast glacier flow in the southwest Laurentide Ice Sheet. *Journal of Quaternary Science: Published for the Quaternary Research Association*, 23(3), pp.249-272
- Evans, D.J.A, Lemmen, D.S. and Rea, B.R., 1999. Glacial landsystems of the southwest Laurentide Ice Sheet: modern Icelandic analogues. *Journal of Quaternary Science*, 14(7), pp.673-691
- Evans, D.J.A., Storrar, R.D. and Rea, B.R., 2016. Crevasse-squeeze ridge corridors: diagnostic features of late-stage palaeo-ice stream activity. *Geomorphology*, 258, pp.40-50
- 1200 Evans, D.J.A., Smith, I.R., Gosse, J.C., and Galloway, J.M., 2021. Glacial landforms and sediments (landsystem) of the Smoking Hills area, Northwest Territories, Canada: Implications for regional Pliocene-Pleistocene Laurentide Ice Sheet dynamics. *Quaternary Science Reviews*, 262, 106958. <https://doi.org/10.1016/j.quascirev.2021.106958>.
- Fulton, R. J. 1995. *Surficial materials of Canada*, Ottawa, Ontario: Geological Survey of Canada. “A” Series Map, 1880A, Scale 1:5,000,000
- 1205 Gandy, N., Gregoire, L.J., Ely, J.C., Cornford, S.L., Clark, C.D. and Hodgson, D.M., 2019. Exploring the ingredients required to successfully model the placement, generation, and evolution of ice streams in the British-Irish Ice Sheet. *Quaternary Science Reviews*, 223, p.105915
- Gomez, N., Gregoire, L.J., Mitrovica, J.X. and Payne, A.J., 2015. Laurentide-Cordilleran Ice Sheet saddle collapse as a contribution to meltwater pulse 1A. *Geophysical Research Letters*, 42(10), pp.3954-3962
- 1210 Greenwood, S. L., Clason, C. C., Helanow, C., & Margold, M., 2016. Theoretical, contemporary observational and palaeo-perspectives on ice sheet hydrology: Processes and products. *Earth-Science Reviews*, 155, pp. 1–27. <https://doi.org/10.1016/j.earscirev.2016.01.010>.
- Greenwood, S.L., and Clark, C.D., 2009. Reconstructing the last Irish Ice Sheet 1: changing flow geometries and ice flow dynamics deciphered from the glacial landform record. *Quaternary Science Reviews*, 28 (27-28), 3085-3100. <https://doi.org/10.1016/j.quascirev.2009.09.008>.
- 1215 Greenwood, S.L., Clark, C.D., and Hughes, A.L.C., 2007. Formalising an inversion methodology for reconstructing ice-sheet retreat patterns from meltwater channels: application to the British Ice Sheet. *Journal of Quaternary Science*, 22 (6), 637-645. <https://doi.org/10.1002/jqs.1083>.



- 1220 Gregoire, L.J., Otto-Bliesner, B., Valdes, P.J. and Ivanovic, R., 2016. Abrupt Bølling warming and ice saddle collapse contributions to the Meltwater Pulse 1a rapid sea level rise. *Geophysical research letters*, 43(17), pp.9130-9137
- Gregoire, L.J., Payne, A.J. and Valdes, P.J., 2012. Deglacial rapid sea level rises caused by ice-sheet saddle collapses. *Nature*, 487(7406), pp.219-222
- Hagedorn, G.W., Smith, I.R., Paulen, R.C., and Ross, M., 2022. *Surficial geology, Enterprise, Northwest Territories, NTS 85-1225 C/9, 10, 15, and 16*; Geological Survey of Canada, Canadian Geoscience Map 438, scale 1:100 000. <https://doi.org/10.4095/328292>
- Hagedorn, G.W., 2022. *Paleo-Ice Sheet and Deglacial History of the Southwestern Great Slave Lake Area* (Master's thesis, University of Waterloo).
- Hebrand, M., and Åmark, M., 1989. Esker formation and glacier dynamics in eastern Skane and adjacent areas, southern 1230 Sweden. *Boreas*, 18(1), pp. 67–81. <https://doi.org/10.1111/j.1502-3885.1989.tb00372.x>.
- Hodder, T.J., Ross, M. and Menzies, J., 2016. Sedimentary record of ice divide migration and ice streams in the Keewatin core region of the Laurentide Ice Sheet. *Sedimentary Geology*, 338, pp.97-114.
- Hughes, A.L.C., Clark, C.D., and Jordan, C.J., 2014. Flow-pattern evolution of the last British ice sheet. *Quaternary Science Reviews* 89, 148-168. <https://doi.org/10.1016/j.quascirev.2014.02.002>.
- 1235 Hughes, O.L., 1987. Late Wisconsinan Laurentide glacial limits of northwestern Canada: the Tutsieta Lake and Kelly Lake phases. Geological Survey of Canada, Paper 85-25, 1987, 19 pages (1 sheet), <https://doi.org/10.4095/122385>
- Hughes, O.L., 1972. Surficial geology of northern Yukon Territory and northwestern District of Mackenzie, Northwest Territories, Geological Survey of Canada, Paper 69–36.
- Hughes, O.L., Hodgson, D.A. (1972) Quaternary reconnaissance northwest District of Mackenzie (106 I, J, K, M, N, O). 1240 Report of activities, part A: April to October, 1971; by Blackadar, R G (ed.); Geological Survey of Canada; Geological Survey of Canada, Paper no. 72-1A, 1972 p. 165-166, <https://doi.org/10.4095/105370>
- Jackson Jr, L.E., Phillips, F.M., Shimamura, K. and Little, E.C., 1997. Cosmogenic ³⁶Cl dating of the Foothills erratics train, Alberta, Canada. *Geology*, 25(3), pp.195-198
- Kamb, B., 2001. Basal zone of the West Antarctic ice streams and its role in lubrication of their rapid motion. *The West 1245 Antarctic ice sheet: behavior and environment*, 77, pp.157-199
- Kennedy, K.E., Froese, D.G., Zazula, G.D. and Lauriol, B., 2010. Last Glacial Maximum age for the northwest Laurentide maximum from the Eagle River spillway and delta complex, northern Yukon. *Quaternary Science Reviews*, 29(9-10), pp.1288-1300
- King, E.C., Hindmarsh, R.C. and Stokes, C.R., 2009. Formation of mega-scale glacial lineations observed beneath a West 1250 Antarctic ice stream. *Nature Geoscience*, 2(8), pp.585-588
- Klassen, R. W., 1971. *Surficial geology, Franklin Bay and Brock River, District of Mackenzie, Northwest Territories*. Geological Survey of Canada Open File 48. <https://doi.org/10.4095/129145>.



- Kleman, J. and Glasser, N.F., 2007. The subglacial thermal organisation (STO) of ice sheets. *Quaternary Science Reviews*, 26(5-6), pp.585-597
- 1255 Kleman, J. and Hättestrand, C., 1999. Frozen-bed Fennoscandian and Laurentide ice sheets during the Last Glacial Maximum. *Nature*, 402(6757), pp.63-66
- Kleman, J., 1990. On the use of glacial striae for reconstruction of paleo-ice sheet flow patterns. *Geografiska Annaler. Series A. Physical Geography*, pp.217-236
- Kleman, J., and Borgström, 1996. Reconstruction of palaeo-ice sheets: the use of geomorphological data. *Earth surface processes and landforms* 21, 893 – 909. [https://doi.org/10.1002/\(SICI\)1096-9837\(199610\)21:10<893::AID-ESP620>3.0.CO;2-U](https://doi.org/10.1002/(SICI)1096-9837(199610)21:10<893::AID-ESP620>3.0.CO;2-U).
- 1260 Kleman, J., Hättestrand, C. and Clarhäll, A., 1999. Zooming in on frozen-bed patches: scale-dependent controls on Fennoscandian ice sheet basal thermal zonation. *Annals of Glaciology*, 28, pp.189-194
- Kleman, J., Hättestrand, C., Borgström, I., and Stroeven, A., 1997. Fennoscandian Palaeoglaciology reconstructed using a glacial geological inversion model. *Journal of Glaciology*, 43 (144), 283-299. <https://doi.org/10.3189/S0022143000003233>.
- 1265 Kleman, J., Hättestrand, C., Stroeven, A.P., Jansson, K.N., De Angelis, H., and Borgström, I., 2006. Reconstruction of palaeo-ice sheets - inversion of their glacial geomorphological record. In: Knight, P.G. (Ed.), *Glacier Science and Environmental Change*. Blackwell Publishing Ltd. <https://doi.org/10.1002/9780470750636.ch38>.
- Kleman, J., Jansson, K., De Angelis, H., Stroeven, A.P., Hättestrand, C., Alm, G. and Glasser, N., 2010. North American Ice Sheet build-up during the last glacial cycle, 115–21 kyr. *Quaternary Science Reviews*, 29(17-18), pp.2036-2051
- 1270 Lakeman, T.R., Pieńkowski, A.J., Nixon, F.C., Furze, M.F., Blasco, S., Andrews, J.T. and King, E.L., 2018. Collapse of a marine-based ice stream during the early Younger Dryas chronozone, western Canadian Arctic. *Geology*, 46(3), pp.211-214
- Lambeck, K., Rouby, H., Purcell, A., Sun, Y. and Sambridge, M., 2014. Sea level and global ice volumes from the Last Glacial Maximum to the Holocene. *Proceedings of the National Academy of Sciences*, 111(43), pp.15296-15303
- 1275 Laskar, J., Robutel, P., Joutel, F., Gastineau, M., Correia, A.C. and Levrard, B., 2004. A long-term numerical solution for the insolation quantities of the Earth. *Astronomy & Astrophysics*, 428(1), pp.261-285
- Lemmen, D.S., Duk-Rodkin, A., and Bednarski, J.M., 1994. Late glacial drainage systems along the northwestern margin of the Laurentide Ice Sheet. *Quaternary Science Reviews* 13 (9-10), 805-828. [https://doi.org/10.1016/0277-3791\(94\)90003-5](https://doi.org/10.1016/0277-3791(94)90003-5).
- Levson, V.M. and Rutter, N.W., 1996. Evidence of Cordilleran late Wisconsinan glaciers in the 'ice-free corridor'. *Quaternary International*, 32, pp.33-51
- 1280 Livingstone, S.J., Storrar, R.D., Hillier, J.K., Stokes, C.R., Clark, C.D. and Tarasov, L., 2015. An ice-sheet scale comparison of eskers with modelled subglacial drainage routes. *Geomorphology*, 246, pp.104-112
- Lowdon, J.A. and Blake, W. (1981) *Geological Survey of Canada Radiocarbon Dates XXII*, Geological Survey of Canada Paper 81-7, 22 p.



- 1285 Lowell, T.V., Kelly, M.A., Howley, J.A., Fisher, T.G., Barnett, P.J., Schwart, R., Zimmerman, S.R., Norris, N. and Malone, A.G., 2021. Near-constant retreat rate of a terrestrial margin of the Laurentide Ice Sheet during the last deglaciation. *Geology*, 49(12), pp.1511-1515
- Mäkinen, J., 2003. Time-transgressive deposits of repeated depositional sequences within interlobate glaciofluvial (esker) sediments in Köyliö, SW Finland. *Sedimentology*, 50(2), pp.327-360
- 1290 Mangerud, J. (2021). The discovery of the Younger Dryas, and comments on the current meaning and usage of the term. *Boreas*, 50, 1-5.
- Mannerfelt, C. M., 1949. Marginal drainage channels as indicators of the gradients of Quaternary ice caps. *Geografiska Annaler*, 31, pp. 194–199.
- Margold, M., Stokes, C.R. and Clark, C.D., 2015a. Ice streams in the Laurentide Ice Sheet: Identification, characteristics and comparison to modern ice sheets. *Earth-Science Reviews*, 143, pp.117-146
- 1295 Margold, M., Stokes, C.R. and Clark, C.D., 2018. Reconciling records of ice streaming and ice margin retreat to produce a palaeogeographic reconstruction of the deglaciation of the Laurentide Ice Sheet. *Quaternary science reviews*, 189, pp.1-30
- Margold, M., Stokes, C.R., Clark, C.D. and Kleman, J., 2015b. Ice streams in the Laurentide Ice Sheet: a new mapping inventory. *Journal of Maps*, 11(3), pp.380-395
- 1300 Menounos, B., Goehring, B.M., Osborn, G., Margold, M., Ward, B., Bond, J., Clarke, G.K., Clague, J.J., Lakeman, T., Koch, J. and Caffee, M.W., 2017. Cordilleran Ice Sheet mass loss preceded climate reversals near the Pleistocene Termination. *Science*, 358(6364), pp.781-784
- Murton, J. B., Bateman, M. D., Waller, R. I., and Whiteman, C. A., 2015. Late Wisconsin glaciation of Hadwen and Summer islands, Tuktoyaktuk Coastlands, NWT, Canada, *GEOQuébec2015*, 7th Canadian Permafrost Conference, pp. 20–23.
- 1305 Norris, S.L., Margold, M., Evans, D.J.A., Atkinson, N. and Froese, D.G., 2023. Dynamical response of the southwestern Laurentide Ice Sheet to rapid Bølling-Allerød warming. *The Cryosphere* 2023, pp.1-32
- Norris, S.L., Tarasov, L., Monteath, A.J., Gosse, J.C., Hidy, A.J., Margold, M. and Froese, D.G., 2022. Rapid retreat of the southwestern Laurentide Ice Sheet during the Bølling-Allerød interval. *Geology*, 50(4), pp.417-421
- Paulen, R.C., & Smith, I.R. 2022. *Surficial geology, Sulphur Bay, Western Great Slave Lake, Northwest Territories, NTS 85-G*. Geological Survey of Canada, Canadian Geoscience Map 443, scale:125,000. <https://doi.org/10.4095/330073>
- 1310 Piasecka, E.D., Stokes, C.R., Winsborrow, M.C. and Andreassen, K., 2018. Relationship between mega-scale glacial lineations and iceberg ploughmarks on the Bjørnøyrenna Palaeo-Ice Stream bed, Barents Sea. *Marine Geology*, 402, pp.153-164
- Pico, T., Robel, A., Powell, E., Mix, A.C. and Mitrovica, J.X., 2019. Leveraging the rapid retreat of the Amundsen Gulf ice stream 13,000 years ago to reveal insight into North American deglaciation. *Geophysical Research Letters*, 46(21), pp.12101-12107
- 1315 Porter, C., Morin, P., Howat, I., Noh, M. J., Bates, B., Peterman, K., Keeseey, S., Schlenk, M., Gardiner, J., Tomko, K., Willis, M., Kelleher, C., Cloutier, M., Husby, E., Foga, S., Nakamura, H., Platson, M., Wethington, M., Williamson, C., Bojesen, M. (2018). ArcticDEM. Available at <https://doi.org/10.7910/DVN/OHHUKH>. Harvard Dataverse, V1. Accessed on 1 April 2021



- 1320 Praetorius, S.K. and Mix, A.C., 2014. Synchronization of North Pacific and Greenland climates preceded abrupt deglacial warming. *Science*, 345(6195), pp.444-448
- Prest, V.K., Grant, D.R., and Rampton, V.N., 1968. *Glacial map of Canada*; Geological Survey of Canada, Map 1253A. doi:10.4095/108979
- Quiquet, A., Dumas, C., Paillard, D., Ramstein, G., Ritz, C. and Roche, D.M., 2021. Deglacial ice sheet instabilities induced by proglacial lakes. *Geophysical Research Letters*, 48(9), p.e2020GL092141.
- 1325 Rampton, V.N., 1982. *Quaternary geology of the Yukon coastal plain*. Geological Survey of Canada, Bulletin 317, 49p.
- Rampton, V.N., 1988. *Quaternary geology of the Tuktoyaktuk coastlands, Northwest Territories*. Geological Survey of Canada, Memoir 423, 1988, 98 pages, <https://doi.org/10.4095/126937>.
- Rasmussen, S.O., Bigler, M., Blockley, S.P., Blunier, T., Buchardt, S.L., Clausen, H.B., Cvijanovic, Dahl-Jensen, D.I., Johnsen, S.J., Fischer, H. and Gkinis, V., 2014. A stratigraphic framework for abrupt climatic changes during the Last Glacial period based on three synchronized Greenland ice-core records: refining and extending the INTIMATE event stratigraphy. *Quaternary Science Reviews*, 106, pp.14-28
- 1330 Rea, B.R., Pellitero, R., Spagnolo, M., Hughes, P., Ivy-Ochs, S., Renssen, H., Ribolini, A., Bakke, J., Lukas, S. and Braithwaite, R.J., 2020. Atmospheric circulation over Europe during the Younger Dryas. *Science Advances*, 6(50), p.eaba4844
- Reyes, A.V., Carlson, A.E., Milne, G.A., Tarasov, L., Reimink, J.R. and Caffee, M.W., 2022. Revised chronology of northwest Laurentide ice-sheet deglaciation from 10Be exposure ages on boulder erratics. *Quaternary Science Reviews*, 277, p.107369
- 1335 Riedel, M., Dallimore, S., Wamstecker, M., Taylor, G., King, E.L., Rohr, K.M., Hong, J.K. and Jin, Y.K., 2021. Mega-scale glacial lineations formed by ice shelf grounding in the Canadian Beaufort Sea during multiple glaciations. *Earth Surface Processes and Landforms*, 46(8), pp.1568-1585
- Ritchie, J.C., 1977. The modern and late Quaternary vegetation of the Campbell-Dolomite uplands, near Inuvik, NWT, Canada. *Ecological Monographs*, 47(4), pp.401-423.
- 1340 Robel, A.A. and Tziperman, E., 2016. The role of ice stream dynamics in deglaciation. *Journal of Geophysical Research: Earth Surface*, 121(8), pp.1540-1554
- Rutter, N. W., Minning, G. V., & Netteville, J. A. (1980). *Surficial geology and geomorphology, Mills Lake, District of Mackenzie*. Geological Survey of Canada, Preliminary Map 15-1978. <https://doi.org/10.4095/109708>.
- 1345 Rutter, N. W., Hawes, R. J., & Catto, N. R. (1993). *Surficial geology, southern Mackenzie River valley, District of Mackenzie, Northwest Territories*. Geological Survey of Canada, Map 1693a. Scale 1:500,000. <https://doi.org/10.4095/193343>
- Sapera, J., 2023. *Glacial dynamics and stratigraphy in the southern Great Slave Lake region, Northwest Territories*. (Master's thesis, Brock University).
- 1350 Scherrenberg, M., Berends, C. and van de Wal, R., 2023. Late Pleistocene glacial terminations accelerated by proglacial lakes. *Climate of the Past Discussions*, 2023, pp.1-30
- Seguinot, J., Rogozhina, I., Stroeven, A.P., Margold, M. and Kleman, J., 2016. Numerical simulations of the Cordilleran ice sheet through the last glacial cycle. *The Cryosphere*, 10(2), pp.639-664



- Seierstad, I.K., Abbott, P.M., Bigler, M., Blunier, T., Bourne, A.J., Brook, E., Buchardt, S.L., Buizert, C., Clausen, H.B., Cook, E. and Dahl-Jensen, D., 2014. Consistently dated records from the Greenland GRIP, GISP2 and NGRIP ice cores for the past 1355 104 ka reveal regional millennial-scale $\delta^{18}O$ gradients with possible Heinrich event imprint. *Quaternary Science Reviews*, 106, pp.29-46
- Shabtaie, S. and Bentley, C.R., 1987. West Antarctic ice streams draining into the Ross Ice Shelf: configuration and mass balance. *Journal of Geophysical Research: Solid Earth*, 92(B2), pp.1311-1336
- Sharpe, D.R., Lesemann, J.E., Knight, R.D. and Kjarsgaard, B.A., 2021. Regional stagnation of the western Keewatin ice sheet 1360 and the significance of meltwater corridors and eskers, northern Canada. *Canadian Journal of Earth Sciences*, 58(10), pp.1005-1026
- Shaw, J., Sharpe, D.R. and Harris, J., 2010. A flowline map of glaciated Canada based on remote sensing data. *Canadian Journal of Earth Sciences*, 47(1), pp.89-101
- Shilts, W.W., 1985. Geological models for the configuration, history and style of disintegration of the Laurentide Ice 1365 Sheet. *Models in Geomorphology*, Edited by MJ Waldenberg. Allen and Unwin, Boston, pp.73-91
- Shilts, W.W., Cunningham, C.M. and Kaszycki, C.A., 1979. Keewatin Ice Sheet—Re-evaluation of the traditional concept of the Laurentide Ice Sheet. *Geology*, 7(11), pp.537-541
- Shreve, R.L., 1985. Esker characteristics in terms of glacier physics, Katahdin esker system, Maine. *Geological Society of America Bulletin*, 96(5), pp.639-646
- 1370 Siegert, M.J., Taylor, J., Payne, A.J. and Hubbard, B., 2004. Macro-scale bed roughness of the Siple Coast ice streams in West Antarctica. *Earth Surface Processes and Landforms: The Journal of the British Geomorphological Research Group*, 29(13), pp.1591-1596
- Smith, D.G., 1992. Glacial Lake Mackenzie, Mackenzie Valley, Northwest Territories, Canada. *Canadian Journal of Earth Sciences*, 29(8), pp.1756-1766
- 1375 Smith, D.G., 1994. Glacial Lake McConnell: paleogeography, age, duration, and associated river deltas, Mackenzie River basin, western Canada. *Quaternary Science Reviews*, 13(9-10), pp.829-843
- Smith, I.R., Deblonde, C., Hagedorn, G. and Paulen, R.C., 2022. A drift isopach model for the southwestern Great Slave Lake region, Northwest Territories, Canada. *Journal of Maps*, pp.1-12
- Smith, I.R., Paulen, R.C., Hagedorn, G.W. 2021. *Surficial geology, northeastern Cameron Hills, Northwest Territories, NTS* 1380 85-C/3, 4, 5, and 6. Geological Survey of Canada, Canadian Geoscience Map 431. <https://doi.org/10.4095/328129>
- Spear, R.W., 1993. The palynological record of Late-Quaternary arctic tree-line in northwest Canada. *Review of Palaeobotany and Palynology*, 79(1-2), pp.99-111
- Stoker, B.J., Livingstone, S.J., Barr, I.D., Ruffell, A., Storrar, R.D. and Roberson, S., 2021. Variations in esker morphology and internal architecture record time-transgressive deposition during ice margin retreat in Northern Ireland. *Proceedings of the* 1385 *Geologists' Association*, 132(4), pp.409-425



- Stoker, B.J., Margold, M., Gosse, J.C., Hidy, A.J., Monteath, A.J., Young, J.M., Gandy, N., Gregoire, L.J., Norris, S.L. and Froese, D., 2022. The collapse of the Cordilleran–Laurentide ice saddle and early opening of the Mackenzie Valley, Northwest Territories, Canada, constrained by 10 Be exposure dating. *The Cryosphere*, 16(12), pp.4865-4886.
- Stokes, C.R. and Clark, C.D., 1999. Geomorphological criteria for identifying Pleistocene ice streams. *Annals of glaciology*, 28, pp.67-74
- 1390 Stokes, C.R. and Clark, C.D., 2003. The Dubawnt Lake palaeo-ice stream: evidence for dynamic ice sheet behaviour on the Canadian Shield and insights regarding the controls on ice-stream location and vigour. *Boreas*, 32(1), pp.263-279.
- Stokes, C.R., 2017. Deglaciation of the Laurentide Ice Sheet from the Last Glacial Maximum. *Cuadernos de Investigación Geográfica*, 43 (2), 377-428.
- 1395 Stokes, C.R., and Clark, C.D., 1999. Geomorphological criteria for identifying Pleistocene ice streams. *Annals of Glaciology* 28, 67 – 74. <https://doi.org/10.3189/172756499781821625>.
- Stokes, C.R., Clark, C.D. and Storrar, R., 2009. Major changes in ice stream dynamics during deglaciation of the north-western margin of the Laurentide Ice Sheet. *Quaternary Science Reviews*, 28(7-8), pp.721-738
- Stokes, C.R., Clark, C.D. and Winsborrow, M.C.M., 2006. Subglacial bedform evidence for a major palaeo-ice stream and its retreat phases in Amundsen Gulf, Canadian Arctic Archipelago. *Journal of Quaternary Science: Published for the Quaternary Research Association*, 21(4), pp.399-412
- 1400 Stokes, C.R., Margold, M., Clark, C.D. and Tarasov, L., 2016. Ice stream activity scaled to ice sheet volume during Laurentide Ice Sheet deglaciation. *Nature*, 530, 322-326.
- Storrar, R. D., Stokes, C. R., and Evans, D. J. A., 2014a. Morphometry and pattern of a large sample (>20,000) of Canadian eskers and implications for subglacial drainage beneath ice sheets. *Quaternary Science Reviews*, 105, pp.1–25. <https://doi.org/10.1016/j.quascirev.2014.09.013>.
- 1405 Storrar, R.D., Stokes, C.R. and Evans, D.J., 2014b. Increased channelization of subglacial drainage during deglaciation of the Laurentide Ice Sheet. *Geology*, 42(3), pp.239-242
- Sutherland, J.L., Carrivick, J.L., Gandy, N., Shulmeister, J., Quincey, D.J. and Cornford, S.L., 2020. Proglacial lakes control glacier geometry and behavior during recession. *Geophysical Research Letters*, 47(19), p.e2020GL088865
- 1410 Wetterich, S., Kizyakov, A.I., Opel, T., Grotheer, H., Mollenhauer, G. and Fritz, M., 2023. Ground-ice origin and age on Herschel Island (Qikiqtaruk), Yukon, Canada. *Quaternary Science Advances*, 10, p.100077
- Wilson, J.T., 1939. Eskers northeast of Great Slave Lake. *Transactions of the Royal Society of Canada.*, 33, pp.119-130
- Winsborrow, M.C., Clark, C.D. and Stokes, C.R., 2004. Ice streams of the Laurentide ice sheet. *Géographie physique et Quaternaire*, 58(2), pp.269-280
- 1415 Winsborrow, M.C., Clark, C.D. and Stokes, C.R., 2010. What controls the location of ice streams? *Earth-Science Reviews*, 103(1-2), pp.45-59



- 1420 Young, N.E., Briner, J.P., Miller, G.H., Lesnek, A.J., Crump, S.E., Thomas, E.K., Pendleton, S.L., Cuzzone, J., Lamp, J.,
Zimmerman, S. and Caffee, M., 2020. Deglaciation of the Greenland and Laurentide ice sheets interrupted by glacier advance
during abrupt coolings. *Quaternary Science Reviews*, 229, p.106091
- Zazula, G.D., Duk-Rodkin, A., Schweger, C.E. and Morlan, R.E., 2004. Late Pleistocene chronology of glacial Lake Old Crow
and the north-west margin of the Laurentide Ice Sheet. In *Developments in Quaternary Sciences* (Vol. 2, pp. 347-362). Elsevier
- Zwally, H.J., Abdalati, W., Herring, T., Larson, K., Saba, J. and Steffen, K., 2002. Surface melt-induced acceleration of
Greenland ice-sheet flow. *Science*, 297(5579), pp.218-222

1425